ISSN 1023-9855

Thoracic Medicine

Volume 36 • Number 1 • March 2021

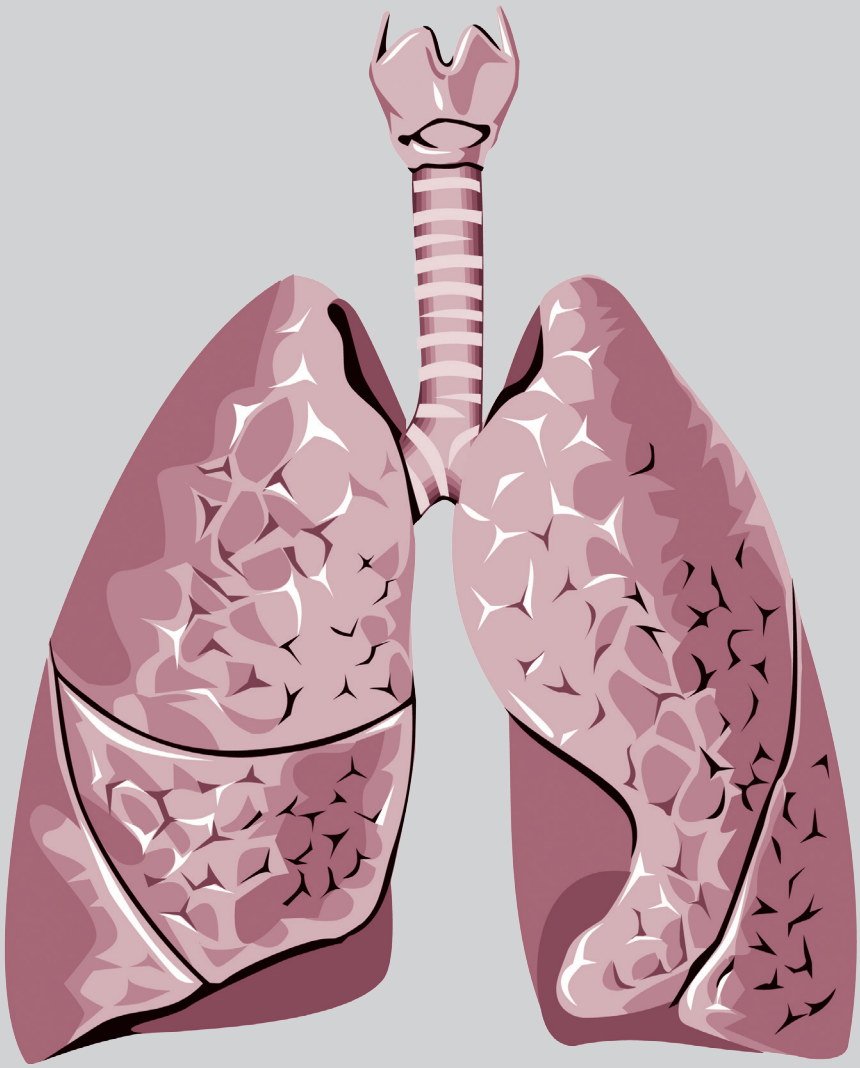

The Official Journal of

Taiwan Society of Pulmonary and Critical Care Medicine

Taiwan Society of Sleep Medicine

Taiwan Society for Respiratory Therapy

Taiwan Society of Tuberculosis and Lung Diseases

Thoracic Medicine

The Official Journal of
Taiwan Society of Pulmonary and Critical Care Medicine
Taiwan Society for Respiratory Therapy
Taiwan Society of Sleep Medicine
Taiwan Society of Tuberculosis and Lung Diseases

Thoracic Medicine

The Official Journal of
Taiwan Society of Pulmonary and Critical Care Medicine
Taiwan Society for Respiratory Therapy
Taiwan Society of Sleep Medicine
Taiwan Society of Tuberculosis and Lung Diseases

Volume 36
Number 1
March 2021

CONTENTS

Different Phenotypes of Respiratory Muscle Strength Influence Exercise Capacity and Health-Related Quality of Life in COPD Patients

Hsiang-Yu Huang[1], Po-Chun Hsieh[2], Mei-Chen Yang[3,4], I-Shiang Tzeng[5], Yao-Kuang Wu[2,3], Chou-Chin Lan[2,3]

Objective: The respiratory muscles are the force that drives respiration. Different phenotypes of respiratory muscle strength (RMS) can have an effect on chronic obstructive pulmonary disease (COPD). However, the effects of phenotypes of RMS on exercise capacity and health-related quality of life (HRQL) are unclear.

Methods: TA total of 85 subjects with stable COPD were included over a 2-year period and comprehensively evaluated by an RMS test, spirometry, cardio-pulmonary exercise test, and St. George's Respiratory Questionnaire (SGRQ). If the maximum inspiratory pressure (MIP) and maximum expiratory pressure (MEP) of the subjects were lower than the cut-off value, this was defined as inspiratory or expiratory muscle weakness. Patients were divided into 4 different phenotypes: type I with normal RMS, type II with inspiratory muscle weakness, type III with expiratory muscle weakness, and type IV with both inspiratory and expiratory muscle weakness. We compared the parameters of exercise capacity, HRQL, and lung function among these phenotypes.

Results: Sixty-one subjects were type I (MIP 74.2±21.8 cmH_2O; MEP 123.2±31.8), 6 were type II (MIP 30.8±4.4 cmH_2O; MEP 96.8±22.9), 10 were type III (MIP 52.8±24.9 cmH_2O; MEP 62.1±8.9 cmH_2O), and 8 were type IV (MIP 32.8±8.1 cmH_2O; MEP 57.9±20.7 cmH_2O). Type IV subjects had the lowest tidal volume (494.2±127.3 ml, $p = 0.002$), highest respiratory rate (27.5±11.4 breaths/min, $p < 0.001$), highest degree of dyspnea, poorest SGRQ and lowest exercise capacity.

Conclusion: RMS is an important factor in dyspnea, exercise capacity and HRQL. Subjects with inspiratory and respiratory failure had more dyspnea, poor exercise capacity and poor HRQL. Health care providers need to be aware of COPD patients with respiratory muscle weakness and carry out early intervention for them. ***(Thorac Med 2021; 36: 1-11)***

Key words: chronic obstructive pulmonary disease; respiratory muscle strength; exercise capacity; health-related quality of life

[1]Division of Respiratory Therapy, Taipei Tzu Chi Hospital, Buddhist Tzu Chi Medical Foundation, New Taipei City, Taiwan, [2]Department of Chinese Medicine, Taipei Tzu Chi Hospital, Buddhist Tzu Chi Medical Foundation, [3]Division of Pulmonary Medicine, Taipei Tzu Chi Hospital, Buddhist Tzu Chi Medical Foundation, New Taipei City, Taiwan, [4]School of Medicine, Tzu-Chi University, Hualien, Taiwan, [5]Department of Research, Taipei Tzu Chi Hospital, Buddhist Tzu Chi Medical Foundation, New Taipei City, Taiwan

Address reprint requests to: Dr. Chou-Chin Lan, Division of Pulmonary Medicine, Taipei Tzu Chi Hospital, Buddhist Tzu Chi Medical Foundation, New Taipei City, Taiwan

289, Jianguo Road, Xindian City, Taipei County 23142, Taiwan, Republic of China

Introduction

Chronic obstructive pulmonary disease (COPD) is a highly prevalent disease worldwide [1]. COPD progressively limits airflow and has a great impact on the patient's ability to be active [1]. Dyspnea, exercise intolerance and poor health-related quality of life (HRQL) are major complaints in subjects with COPD [1-2]. Although obstruction of airflow is the central physiological impairment in COPD, several studies have reported a weak relationship between symptoms and exercise capacity and impairment of lung function [3]. Lung function explains just 28% of dyspnea [3]. To better understand the disability of COPD patients, other factors that lead to symptoms development and exercise intolerance, such as the respiratory muscle functioning, should be considered. However, studies into the role of respiratory muscles in COPD are quite limited.

Respiratory muscles generate pressure differences and drive the forces of respiration, and should be an important clinical issue in COPD. Respiratory muscle weakness (RMW) results in respiratory pump failure and dyspnea [4]. It is rational to postulate that RMW may cause dyspnea, poor HRQL and exertion intolerance. However, the relationship between phenotypes of respiratory muscle functioning and exercise capacity and HRQL is not fully understood.

The respiratory muscle plays an important role in COPD, but the initial symptoms and signs of RMW are often subtle and nonspecific. When RMW becomes obvious, symptoms progress to dyspnea, tachypnea, and paradoxical respiration [5]. In cases of severe RMW, reduced coughing ability may lead to recurrent lung infection [6]. A terminal case of RMW may progress to respiratory failure and ventilator dependence [7]. Therefore, early evaluation of respiratory muscle strength (RMS) should be a part of the assessment of subjects with COPD.

Maximal inspiratory pressure (MIP) indicates the strength of the diaphragm and other inspiratory muscles, whereas maximal expiratory pressure (MEP) indicates the strength of abdominal and intercostal muscles [8]. The measurement of RMS (MIP and MEP) is a simple, rapid, and non-invasive test, and of high value in excluding clinically significant RMW [8].

Although, RMS is important in patients with COPD and the measurement of RMS is non-invasive and simple, it is not widely measured in clinical settings. For this study, we investigated the roles of RMS in subjects with COPD. Through comprehensive assessment of RMS, spirometry, exercise capacity and HRQL, we aimed to gain a clear understanding of the importance of RMS in COPD.

Materials and Methods

Patient recruitment

A total of 85 subjects with stable COPD were recruited from the outpatient clinic at our hospital from January 1, 2016 to December 31, 2017. The inclusion criteria were as follows: (1) a diagnosis of COPD based on the Global Initiative for Chronic Obstructive Lung Disease (GOLD) guideline [9]; (2) no acute exacerbations for more than 3 months before recruitment; and (3) the ability to complete the exercise test. The ethics committee of Taipei Tzu-Chi Hospital approved the research protocol.

Respiratory muscle strength (RMS)

Tests for RMS, including the measurement of MIP and MEP, were assessed using a

standard mouthpiece and a direct dial pressure gauge (Respiratory Pressure Meter, Micro Medical Corp, England). When these measurements were taken, the patients had not undergone previous exercise training or inspiratory muscle straining.

Measurements were taken with the subjects in a sitting position with a nose clip. MIP was measured from residual volume. The subjects were asked to exhale to a residual volume and then make a rapid, maximal inspiratory effort, sustained for 1–2 seconds. MEP was measured from total lung capacity. Subjects were asked to inspire to total lung capacity and then make a rapid and maximal expiratory effort, sustained for 1–2 seconds. MIP and MEP were measured several times, and after 5 attempts, the plateau of values showed relatively little variability (10% of reading). The highest values were recorded [10]. The cut-off values were derived from Wilson *et al*., who determined MIP and MEP prediction utilizing stepwise multiple regression analysis [11]. Prediction equations for MIP and MEP in adults were:

For males, MIP = 142 − (1.03 × Age); MEP = 180 − (0.91 × Age)

For females, MIP = -43 + (0-71 × Height); MEP = 3.5 + (0.55 × Height)

Age is in years, and height is in centimeters.

MIP (%) = measured MIP/predicted MIP.

MEP (%) = measured MEP/predicted MEP.

Steier *et al*. utilized the data in that study to define the cut-off values by subtracting 1.96 standard deviations from the mean of a normal population8. The normal cut-off values for MIP were 45 cmH_2O for males and 30 cmH_2O for females, and inspiratory muscle weakness was indicated in patients with values below these cut-off levels [11]. The normal cut-off values for MEP were 80 cmH_2O for males and 60 cmH_2O for females, and expiratory muscle weakness was indicated in patients with values below the cut-off levels [11]. Patients were divided into 4 different phenotypes: type I with normal MIP and MEP, type II with inspiratory muscle weakness, type III with expiratory muscle weakness, and type IV with both inspiratory and expiratory muscle weakness.

Pulmonary function test

All subjects underwent a pulmonary function test with a spirometer (Medical Graphics Corporation; St Paul, MN, USA), in accordance with the standards of the American Thoracic Society [12]. The degree of airflow obstruction was assessed by forced expiratory volume in 1 second (FEV_1) % according to GOLD guidelines [9].

Cardiopulmonary exercise test

The cardiopulmonary exercise test (CPET) was performed as an incremental, symptom-limited test on an electronically braked cycle ergometer (Lode Corival, the Netherlands). The MedGraphics cardiopulmonary diagnostic system (Breeze suite 6.1, Medical Graphics Corporation; St Paul, MN, USA) was used to analyze the expired air breath-by-breath with output of oxygen uptake (VO_2), carbon dioxide output (VCO_2), respiratory rate (RR), tidal volume (V_T), and end tidal PCO_2 ($PETCO_2$). In addition, we continuously monitored the electrocardiogram, hemoglobin saturation by pulse oximeter (SpO_2), and blood pressure (BP). The test consisted of measurements during 2 minutes of rest, followed by 2 minutes of unloaded pedaling and a ramp increase of load (increments of 10 watts/minute) to maximal workload. Subjects were encouraged to do their best and to

achieve maximal possible performance. Minute ventilation ($VE=V_T*RR$) and oxygen pulse ($O_2P=VO_2/HR$) were calculated by the system. The anaerobic threshold (AT) was determined by VCO_2 vs VO_2 plot [13].

Health-related quality of life

HRQL was assessed by the validated Chinese-language version of St. George's Respiratory Questionnaire (SGRQ) [14]. The SGRQ is a respiratory disease-specific questionnaire. Four components (total, symptoms, activity, and impact) were included and scores ranged from 100 (worst) to 0 (best) [14].

Dyspnea score

Ratings of dyspnea were evaluated at rest and at the end of the exercise test. The dyspnea score was evaluated by a 10-point Borg scale [15]. Higher dyspnea scores indicated more dyspnea [15]. For every individual reaching different maximal work rates, the dyspnea score was assessed at different workloads, and the level of iso-work dyspnea was calculated by dividing the exertional dyspnea score by the workload (watt).

Statistical analysis

All parameters were expressed as mean ± standard deviation (SD). One-way analysis of variance (ANOVA) was used to compare the parameters among the 4 types of RMS. Post-hoc analysis followed by least significant difference (LSD) in the case of significant differences ($p < 0.05$) showed in the ANOVA results. Pearson's chi-square was used to compare gender and smoking status. All statistical analyses were performed using SPSS version 18.0 (SPSS, Inc., Chicago, IL).

We performed a correlation analysis to evaluate the relationship between RMS, exercise capacity (VO_2 max), and HRQoL while controlling for potential confounding variables including age, smoking status, and body mass index.

Results

Anthropometric characteristics of the 4 types (Table 1)

A total of 85 subjects were included in this study. The clinical characteristics are shown in (Table 1). Age, body weight, body height and smoking status presented no significant differences among the 4 types.

Respiratory muscle strength, spirometric and ventilatory parameters among the 4 types (Table 2)

The subjects were grouped into 1 of the 4 types based on MIP and MEP. Sixty-one subjects were type I (MIP 74.2±21.8 cmH_2O; MEP 123.2±31.8), 6 were type II (MIP 30.8±4.4 cmH_2O; MEP 96.8±22.9), 10 were type III (MIP 52.8±24.9 cmH_2O; MEP 62.1±8.9 cmH_2O), and 8 were type IV (MIP 32.8±8.1 cmH_2O; MEP 57.9±20.7 cmH_2O). Lower MIP was observed in types II and IV ($p<0.001$), and lower MEP was observed in types III and IV ($p<0.001$).

Forced vital capacity (FVC) was not significantly different among the 4 types ($p = 0.055$). However, FEV_1 was lower in types III (0.80±0.23 L/min) and IV (0.75±0.12 L/min) than in types I (1.13±0.44 L/min) and II (1.16±0.60 L/min) ($p = 0.018$).

At rest, the type IV subjects displayed the lowest V_T (494.2±127.3 ml) ($p = 0.002$) and highest RR (27.5±11.4 breaths/min) ($p < 0.001$). At peak exercise, V_T was also the lowest in type IV (688.7±252.1 ml) ($p< 0.001$).

Table 1. Baseline Characteristics

	Type I (n= 61)	Type II (n=6)	Type III (n= 10)	Type IV (n= 8)	*p*
Age (yrs)	69.1±9.0	71.5±3.0	75.7±6.9	68.8±11.4	0.170
BH (cm)	162.6±8.0	160.5±8.4	161.5±8.1	159.1±4.8	0.633
BW(kg)	61.8±11.7	55.8±8.6	58.5±12.5	49.5±10.5*	0.034
BMI (kg/cm^2)	23.3±3.6	21.4±4.0	22.4±4.5	19.5±3.6*	0.048
Smoking status					
Non-smoker	8	2	1	2	0.083
Current smoker	20	2	8	3	
Ex-smoker	33	2	1	3	

* $p < 0.05$ as compared with Type I, †p < 0.05 as compared with type II, ‡p < 0.05 as compared with type III

Acronyms: BH, body height; BW, body weight; BMI, body mass index.

Table 2. Respiratory Parameters

	Type I (n= 61)	Type II (n=6)	Type III (n= 10)	Type IV (n= 8)	*p*
MIP (cmH_2O)	74.2±21.8	30.8±4.4*	52.8±24.9	32.8±8.1*	<0.001
MIP (%)	75.3±22.3	34.5±7.2*	53.8±23.3	33.8±6.1*	<0.001
MEP (cmH_2O)	123.2±31.8	96.8±22.9	62.1±8.9*	57.9±20.7*	<0.001
MEP (%)	67.1±17.3	56.5±23.3	34.1±5.4*†	32.1±1.0*†	<0.001
FVC (L)	2.31±0.68	1.92±0.84	1.90±0.61	1.74±0.71	0.055
FVC (% predicted)	82.4±18.7	69.9±16.3	72.0±16.8	69.8±27.0	0.100
FEV_1 (L/min)	1.13±0.44	1.16±0.60	0.80±0.23*	0.75±0.12*	0.018
FEV_1 (% predicted)	51.6±17.3	53.3±17.9	40.4±13.2*	38.3±6.6*	0.049
FEV_1/FVC (%)	49.2±11.6	59.4±11.0	44.7±17.7	49.9±22.4	0.224
VE rest (L/min)	12.4±3.3	11.0±3.2	11.0±3.0	12.5±1.9	0.421
VE exercise (L/min)	34.5±9.9	34.5±18.2	26.2±6.7*	24.4±3.3*	0.010
RR rest (breaths/min)	18.5±4.4	18.8±2.6	19.7±4.8	27.5±11.4*†‡	<0.001
RR exercise (breaths/min)	32.2±7.7	34.3±6.9	32.7±6.7	38.0±10.7	0.258
V_T rest (ml)	685.0±151.6	592.5±186.9	563.4±117.3*	494.2±127.3*	0.002
V_T exercise (ml)	1094.0±292.2	978.4±384.5	818.4±219.8*	688.7±252.1*	0.001

* $p < 0.05$ as compared with Type I, †p < 0.05 as compared with type II, ‡p < 0.05 as compared with type III

Acronyms: MIP, maximal inspiratory pressure; MEP, maximal expiratory pressure; FVC, forced vital capacity; FEV_1, forced expiratory volume in 1 second; VE, minute ventilation; RR, respiratory rate; V_T, tidal volume.

Exercise capacity among the 4 types (Table 3)

VO_2 and work rate at peak exercise indicated exercise capacity. The type IV subjects displayed the lowest exercise capacity (VO_2 peak 645.0±260.3 ml/min, 53.6±19.3%, $p < 0.05$).

Circulatory parameters among the 4 types (Table 4)

The type IV subjects had the lowest AT (516.9±167.1 ml/min, p=0.040) and O_2P (5.4±1.7 mL/beat, p=0.002). However, mean BP and HR were not significantly different between the 4 types ($p > 0.05$).

Gas exchanges among the 4 types (Table 5)

Gas exchange at rest and peak exercise was assessed by SpO_2 and $PETCO_2$. SpO_2 and $PETCO_2$ at rest and peak exercise were not significantly different among the 4 types ($p > 0.05$).

Dyspnea and health-related quality of life among the 4 types (Table 6)

The type IV subjects had more dyspnea at rest (p=0.013) and iso-work exercise (p=0.007).

Table 3. Exercise Capacity

	Type I (n= 61)	Type II (n=6)	Type III (n= 10)	Type IV (n= 8)	*p*
VO_2 peak (ml/min)	968.2±285.2	908.7±128.9	784.5±174.6*	645.0±260.3*†	0.007
VO_2 peak (%)	66.8±18.3	75.7±10.5	62.8±21.9	53.6±19.3*†	0.013
WR (watt)	67.9±27.6	62.0±19.6	48.2±13.6*	34.1±23.4*†	0.003
WR (%)	73.7±28.8	85.1±17.4	63.0±23.0	43.9±27.3*†	0.018

* $p < 0.05$ as compared with Type I, †p < 0.05 as compared with type II, ‡p < 0.05 as compared with type III.
Acronyms: VO_2, oxygen uptake; WR, work rate.

Table 4. Circulatory Parameters

	Type I (n= 61)	Type II (n=6)	Type III (n= 10)	Type IV (n= 8)	*p*
VO_2 at AT (ml/min)	644.2±136.8	583.8±67.5	556.9±119.5	516.9±167.1*	0.040
O_2P (mL/beat)	7.8±2.0	7.7±1.1	6.0±1.6	5.4±1.7*	0.002
MBP at rest (mmHg)	89.7±10.8	84.8±16.4	82.4±12.5	91.9±9.4	0.188
MBP at exercise (mmHg)	108.5±15.0	99.2±17.0	99.8±105.3	106.3±17.6	0.225
HR at rest (beats/min)	86.8±13.5	89.2±9.9	86.1±10.2	94.1±11.3	0.360
HR at exercise (beats/min)	124.8±16.6	118.8±11.7	131.5±13.2	118.3±20.9	0.320

* $p < 0.05$ as compared with Type I, †p < 0.05 as compared with type II, ‡p < 0.05 as compared with type III.
Acronyms: AT= anaerobic threshold; O_2P= oxygen pulse; MBP= mean blood pressure; HR= heart rate.

Table 5. Gas Exchanges

	Type I (n= 61)	Type II (n=6)	Type III (n= 10)	Type IV (n= 8)	*p*
SpO_2 at rest (%)	96.2±1.9	96.7±2.0	95.0±1.9	94.4±2.3	0.290
SpO_2 at exercise (%)	93.0±3.4	93.5±3.4	92.2±3.7	92.9±4.0	0.213
$PETCO_2$ at rest (mmHg)	34.9±5.2	38.5±7.8	34.9±5.6	34.1±8.0	0.830
$PETCO_2$ at exercise (mmHg)	39.9±6.7	43.8±10.1	42.5±5.4	40.3±12.6	0.760

* $p < 0.05$ as compared with Type I, †p < 0.05 as compared with type II, ‡p < 0.05 as compared with type III.
Acronyms: SpO_2, blood oxygen saturation by pulse oximeter; $PETCO_2$, end tidal carbon dioxide.

Table 6. Dyspnea and Health-Related Quality of Life

	Type I (n= 61)	Type II (n=6)	Type III (n= 10)	Type IV (n= 8)	*p*
Dyspnea, rest	0.4±0.6	0.4±0.8	0.7±0.8	1.1±0.8*†	0.013
Dyspnea, exercise	5.5±1.7	5.2±2.5	6.0±1.3	5.0±0.8	0.593
Iso-work dyspnea (Dyspnea/watt)	0.11±0.12	0.09±0.04	0.13±0.04	0.40±0.66*	0.007
SGRQ, total	45.8±17.7	56.9±10.6	61.1±8.7*	62.5±15.3*	0.004
SGRQ, symptom	55.1±22.3	54.0±8.3	69.4±26.7	74.5±15.6*	0.041
SGRQ, activity	58.0±20.5	73.9±11.6	81.1±11.7*	75.9±19.1*	0.001
SGRQ, impact	36.3±20.0	48.1±19.7	48.7±11.7	51.6±19.1*	0.046

* $p < 0.05$ as compared with Type I, †p < 0.05 as compared with type II, ‡p < 0.05 as compared with type III.
Acronym: SGRQ, St. George's Respiratory Questionnaire.

In addition, the type IV subjects had the poorest SGRQs in terms of symptoms (74.5±15.6, p=0.041), impact (51.6±19.1, p=0.046), activity (75.9±19.1, p=0.001) and total scores (62.5±15.3, p=0.004).

Correlation between respiratory muscle strength vs. exercise capacity and HRQL

The correlation between RMS and exercise capacity (VO_2 peak) and HRQL (SGRQ-total) is shown in (Figure 1). There was a significantly negative partial correlation between SGRQ and MIP as -0.379, with a p value = 0.001, and a significantly negative partial correlation between SGRQ and MEP as -0.401, with a p value < 0.001 (Figure 1B). There was a significantly positive partial correlation between peak VO_2 and MIP as 0.427, with a p value < 0.001, and a significantly positive partial correlation between peak VO_2 and MEP as 0.418, with a p value < 0.001 (Figure 1D). The regression models were summarized as follows:

SGRQ = 86.76 – 0.24×MIP – 0.24×Age + 1.09×smoking – 0.25×BMI

SGRQ = 89.72 – 0.19×MEP – 0.23×Age + 2.61 x smoking – 0.28×BMI

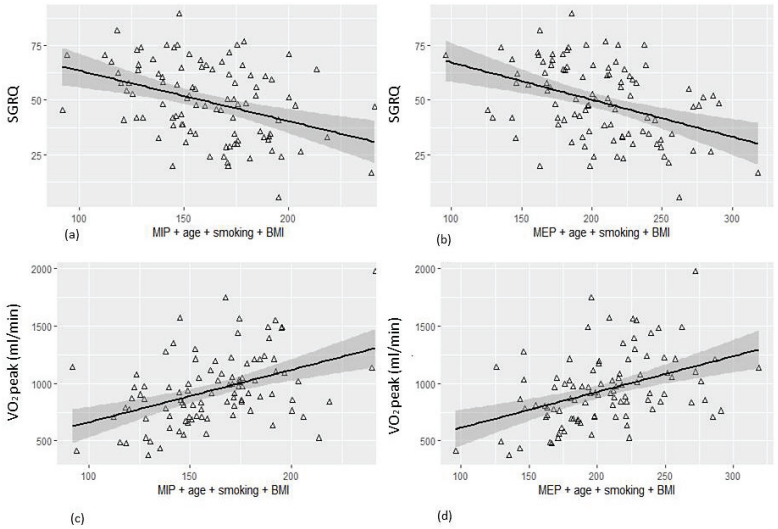

Fig. 1. Correlation between respiratory muscle strength vs. exercise capacity and HRQL. There was a significantly negative partial correlation between SGRQ and MIP (A) as -0.379 with a *p* value = 0, and a significantly negative partial correlation between SGRQ and MEP (B) as -0.401 with a *p* value < 0.001. There was a significantly positive partial correlation between peak VO_2 and MIP (C) as 0.427 with a *p* value < 0.001, and a significantly positive partial correlation between peak VO_2 and MEP (D) as 0.418 with a p value < 0.001.

Peak VO_2 (ml/min) = 329.45+2.46×MIP – 5.60 x Age + 27.62×smoking + 34.83×BMI

Peak VO_2 (ml/min) = 312.87 + 1.72×MEP – 5.77×Age + 15.81×smoking +35.62×BMI

(MIP and MEP in cmH2, Age in years, smoking in pack-years, BMI in kg/m^2).

Discussion

There are some important findings in the current study. The prevalence of RMW was high (approximately 28%) in subjects with COPD in the current study. Subjects with both inspiratory and expiratory muscle weakness had lower V_T, higher RR, more dyspnea, lower AT, lower O_2P, poor HRQL and lower exercise capacity. These results address the important role of RMS in COPD.

The respiratory muscles are important for generating the strength needed to maintain adequate ventilation [16]. Our current study revealed that subjects with both inspiratory and expiratory muscle weakness had the lowest V_T at rest or exercise, poorest HRQL and lowest exercise capacity. When patients have RMW, they cannot generate enough strength to drive ventilation and they often have lower V_T. In order to maintain sufficient minute ventilation with a low V_T, the respiratory rate must be increased, which causes more dyspnea and poorer HRQoL [17]. During exercise, these patients are unable to generate adequate V_T, so this situation will worsen. They therefore will have a more rapid respiratory rate, dyspnea and exercise intolerance [17].

Traditional indications for assessing RMS include the presence of neuromuscular diseases, such as Guillain-Barre syndrome, myasthenia

gravis, amyotrophic lateral sclerosis, and polio [18]. Patients with COPD do not routinely receive testing for RMS. The recognition of RMW is often delayed because its symptoms are nonspecific and subtle in the early stages of the disease. However, as in our study, impairment of RMS affects approximately one-third of subjects with COPD, and lower RMS results in more dyspnea, lower exercise capacity and poor HRQL. Physicians should be aware of this condition and perform testing for RMS in patients with COPD, especially those with dyspnea, poor HRQL and exertion intolerance.

Exercise performance has an affect daily activities and HRQL [19]. RMW is an important factor resulting in exercise limitation [20]. Respiratory muscles generate the pressure differences driving ventilation. Therefore, RMW leads to an inability to generate adequate pressure differences to drive ventilation. RMW, along with increased ventilatory demands during activity or exercise, result in exertional dyspnea and exercise intolerance [20]. Activity-related dyspnea is, therefore, one of the earliest symptoms in patients with COPD [21].

Multiple factors lead to RMW in COPD patients, including airflow obstruction, lung hyperinflation, steroid-induced myopathy, and malnutrition [22]. Airway obstruction leads to increased airway resistance [22]. With RMW, diaphragm and respiratory muscles face increased loads, and greater respiratory muscle forces are required to overcome airway resistance. Chronic overload eventually leads to RMW. This result was similar to that reported by Kim *et al*., in which RMS decreased in more advanced COPD stages [23]. Lung hyperinflation is a cardinal feature in COPD and results in alternations in respiratory muscle tension [22]. In lung hyperinflation, the capacity of the respiratory muscles to generate pressure is decreased due to mechanical disadvantages [24]. The overloading of respiratory muscles further results in muscle fatigue. Furthermore, malnutrition is highly prevalent in COPD patients [25]. Malnutrition further predisposes patients to loss of diaphragm and respiratory muscle mass [22]. COPD is also associated with systemic inflammation [22]. Systemic inflammation and oxidative stress lead to a breakdown of muscle mass and contribute to weakness in the diaphragm and respiratory muscles [22].

We suggest that clinicians should be aware of RMW in patients with COPD, and that this could be an important factor in preventing further disability. There are several treatment modalities that can be used for RMW. For example, inspiratory muscle training using threshold devices has been reported to improve inspiratory muscle strength and exercise capacity HRQL, and to decrease dyspnea [26]. Respiratory muscle rest by means of negative pressure ventilation has been reported to improve exercise tolerance in COPD [27]. A meta-analysis also showed that pulmonary rehabilitation had significant effects on the MIP, MEP and dyspnea scores [28].

Limitations of this study

There are some important findings in the current study. The prevalence of RMW was high (approximately 28%) in subjects with COPD in the current study. Subjects with both inspiratory and expiratory muscle weakness had lower VT, higher RR, more dyspnea, lower AT, lower O_2P, poor HRQL and lower exercise capacity. These results address the important role of RMS in COPD.

Conclusion

RMW has an important effect on subjects with COPD, and can result in more dyspnea, poor HRQL and lower exercise capacity. Strategies for the early recognition of RMW in subjects are important. Physicians should be more aware of the need to perform tests for RMS in subjects with COPD, especially those with dyspnea, poor HRQL and exercise intolerance.

Acknowledgements

This study was supported by grants from Taipei Tzu Chi Hospital, Buddhist Tzu Chi Medical Foundation (TCRD-TPE-106-11 and TCRD-TPE-108-RT-4).

Conflicts of Interest

The authors have no commercial associations or sources of support that might pose a conflict of interest.

References

1. Vogelmeier CF, Criner GJ, Martinez FJ, *et al*. Global Strategy for the Diagnosis, Management, and Prevention of Chronic Obstructive Lung Disease 2017 Report. GOLD Executive Summary. Am J Respir Crit Care Med 2017; 195: 557-82.
2. Lan CC, Chu WH, Yang MC, et al. Benefits of pulmonary rehabilitation in patients with COPD and normal exercise capacity. Respir Care 2013; 58: 1482-8.
3. Johnson KM, Safari A, Tan WC, *et al*. Heterogeneity in the respiratory symptoms of patients with mild-to-moderate COPD. Int J Chron Obstruct Pulmon Dis 2018; 13: 3983-95.
4. Singer J, Yelin EH, Katz PP, *et al*. Respiratory and skeletal muscle strength in chronic obstructive pulmonary disease: impact on exercise capacity and lower extremity function. J Cardiopulm Rehabil Prev 2011; 31: 111-9..
5. Gilmartin JJ, Gibson GJ. Mechanisms of paradoxical rib cage motion in patients with chronic obstructive pulmonary disease. Am Rev Respir Dis 1986; 134: 683-7.
6. Dassios TG, Katelari A, Doudounakis S, *et al*. Chronic Pseudomonas aeruginosa infection and respiratory muscle impairment in cystic fibrosis. Respir Care 2014; 59: 363-70.
7. Adler D, Janssens JP. The pathophysiology of respiratory failure: control of breathing, respiratory load, and muscle capacity. Respiration 2018; 13: 1-12.
8. Steier J, Kaul S, Seymour J, *et al*. The value of multiple tests of respiratory muscle strength. Thorax 2007; 62: 975-80.
9. Song JH, Lee CH, Um SJ, *et al*. Clinical impacts of the classification by 2017 GOLD guideline comparing previous ones on outcomes of COPD in real-world cohorts. Int J Chron Obstruct Pulmon Dis 2017; 13: 3473-84.
10. McConnell AK, Copestake AJ. Maximum static respiratory pressures in healthy elderly men and women: issues of reproducibility and interpretation. Respiration 1999; 66: 251-8.
11. Wilson SH, Cooke NT, Edwards RH, *et al*. Predicted normal values for maximal respiratory pressures in Caucasian adults and children. Thorax 1984; 39: 535-8.
12. Culver BH, Graham BL, Coates AL, *et al*. Recommendations for a Standardized Pulmonary Function Report. An Official American Thoracic Society Technical Statement. Am J Respir Crit Care Med 2017; 196: 1463-72.
13. Lan CC, Yang MC, Huang HC, *et al*. Serial changes in exercise capacity, quality of life and cardiopulmonary responses after pulmonary rehabilitation in patients with chronic obstructive pulmonary disease. Heart Lung 2018; 47: 477-84.
14. Wang KY, Chiang CH, Maa SH, *et al*. Psychometric assessment of the Chinese-language version of the St. George's Respiratory Questionnaire in Taiwanese patients with bronchial asthma. J Formos Med Assoc 2001; 100: 455-60.
15. Cheng ST, Wu YK, Yang MC, *et al*. Pulmonary rehabilitation improves heart rate variability at peak exercise, exercise capacity and health-related quality of life in chronic obstructive pulmonary disease. Heart Lung

2014; 43: 249-55.
16. da Fonsêca JDM, Resqueti VR, Benício K, *et al*. Acute effects of inspiratory loads and interfaces on breathing pattern and activity of respiratory muscles in healthy subjects. Front Physiol 2019; 10: 993.
17. Gilman SA, RB. B Physiologic changes and clinical correlates of advanced dyspnea Curr Opin Support. Palliat Care 2009; 3: 93-7.
18. Polkey MI, Lyall RA, Yang K, *et al*. Respiratory muscle strength as a predictive biomarker for survival in amyotrophic lateral sclerosis. Am J Respir Crit Care Med 2017; 195: 86-95.
19. Bui KL, Nyberg A, Maltais F, *et al*. Functional tests in chronic obstructive pulmonary disease, Part 1: Clinical relevance and links to the international classification of functioning, disability, and health. Ann Am Thorac Soc 2017; 14.
20. Hoffman M, Assis MG, Augusto VM, *et al*. The effects of inspiratory muscle training based on the perceptions of patients with advanced lung disease: a qualitative study. Braz J Phys Ther 2018; 22: 215-21.
21. Ozsoy I, Kahraman BO, Acar S, *et al*. Factors influencing activities of daily living in subjects with COPD. Respir Care 2018; 64: 189-95.
22. Barreiro E, Jaitovich A. Muscle atrophy in chronic obstructive pulmonary disease: molecular basis and potential therapeutic targets. J Thorac Dis 2018; 10: S1415-S24.
23. Kim NS, Seo JH, Ko MH, *et al*. Respiratory muscle strength in patients with chronic obstructive pulmonary disease. Ann Rehabil Med 2017; 41: 659-66.
24. Klimathianaki M, Vaporidi K, Georgopoulos D. Respiratory muscle dysfunction in COPD: from muscles to cell. Curr Drug Targets 2011; 12: 478-88.
25. Lan CC, Su CP, Chou LL, *et al*. Association of body mass index with exercise cardiopulmonary responses in lung function-matched patients with chronic obstructive pulmonary disease. Heart Lung 2012; 41: 374-81.
26. Beaumont M, Forget P, Couturaud F, *et al*. Effects of inspiratory muscle training in COPD patients: A systematic review and meta-analysis. Clin Respir J 2018; 12: 2178-88.
27. Renston JP, DiMarco AF, Supinski GS. Respiratory muscle rest using nasal BiPAP ventilation in patients with stable severe COPD. Chest 1994; 105: 1053-60.
28. Lee EN, Kim MJ. Meta-analysis of the effect of a pulmonary rehabilitation program on respiratory muscle strength in patients with chronic obstructive pulmonary disease. Asian Nurs Res 2018; S1976-1317: 30245-7.

Durable Ceritinib Response in Stage IV Lung Adenocarcinoma Patients Harboring the Anaplastic Lymphoma Kinase Fusion Gene: Long Term Follow-up in a Tertiary Care Medical Center

Hsu-Ching Huang[1,2], Chun-Ming Tsai[3], Chi-Lu Chiang[1,2], Chao-Hua Chiu[1,2]

Introduction: Advanced-stage lung adenocarcinoma patients harboring the anaplastic lymphoma kinase (ALK) fusion gene show a good response to ALK tyrosine kinase inhibitors (TKIs). Ceritinib, the first FDA-approved second-generation ALK TKI, has shown potent effects in clinical trials. Here, we evaluated the long-term clinical outcomes of patients treated with ceritinib.

Methods: We retrospectively reviewed patients who started ceritinib treatment between April 2013 and August 2017. The medical records and diagnostic images of the patients, as well as the local treatment methods, were retrospectively reviewed.

Results: Overall, 23 patients were included and a response rate of 74% was observed. With a median follow-up of 42.1 months, the median progression-free survival was 15 months (95% confidence interval, 11.6-19.5), and median overall survival had not been reached by July 31, 2019. Twelve patients (52.2%) received ceritinib beyond progression, with 8 receiving additional local treatment upon disease progression. Treatment duration after progression ranged between 2.7 and 65.5 months, with a median of 31.4 months.

Conclusion: Ceritinib is well tolerated in clinical settings. Patients with advanced-stage lung adenocarcinoma harboring ALK mutations could achieve favorable long-term outcomes through multimodality treatment. ***(Thorac Med 2021; 36: 12-17)***

Key words: lung adenocarcinoma, anaplastic lymphoma kinase, ceritinib

Introduction

The anaplastic lymphoma kinase (ALK) fusion gene was discovered in 2007 [1], Since then, in-depth studies have gradually defined this specific patient group, which accounts for approximately 5% of lung adenocarcinoma cases across races, as having a relatively younger age and intracranial disease upon diagnosis [2].

With the emergence of crizotinib, the first ALK tyrosine kinase inhibitor (TKI), the overall survival (OS) of this patient group has been

[1]Department of Chest Medicine, Taipei Veterans General Hospital, Taipei, Taiwan;
[2]School of Medicine, National Yang-Ming University, Taipei, Taiwan;
[3]Department of Oncology, Taipei Veterans General Hospital, Taipei, Taiwan.
Address reprint requests to: Dr. Hsu-Ching Huang, Department of Chest Medicine, Taipei Veterans General Hospital; 201, Section 2, Shih-Pai Road, Taipei, 112, Taiwan

significantly prolonged [3]. Nevertheless, inevitable drug resistance has motivated the development of alternative ALK TKIs. Ceritinib (LDK378), the first FDA-approved second-generation ALK TKI, showed potent effects regardless of previous crizotinib treatment [4]. Here, we present a detailed review of our clinical experience with ceritinib.

Methods

Patients

Stage IV lung adenocarcinoma patients enrolled in ceritinib clinical trials (CLDK378A1103, CLDK3782301, and CLDK378A2205) from April 2013 to August 2017 at Taipei Veterans General Hospital were included. The medical records and diagnostic images of the patients, including local treatment methods, were retrospectively reviewed. The final follow-up date was July 31, 2019.

Statistical analysis

Progression-free survival (PFS) was defined as survival until the first occurrence of radiologically confirmed progression based on the Response Evaluation Criteria in Solid Tumors (RECIST), or death. PFS and OS were estimated using the Kaplan-Meier method. Patients who were alive on July 31, 2019 or lost to follow-up were considered censored.

Results

Patient characteristics

A total of 23 patients commenced ceritinib therapy between April 2013 and August 2017. Their demographic characteristics are presented in Table 1. Seven patients had received prior crizotinib treatment, while the remaining 16 pa-

Table 1. Epidemiological Factors and Clinical Variables Stratified by the Presence of Central Sleep Apnea

		All patients, n=23
Age (years)		50 (27-73)
Sex		
	Female	14 (60%)
	Male	9 (40%)
Previous crizotinib use		
	Never	16 (70%)
	Previous crizotinib use	7 (30%)
Treatment line of ceritinib		
	1	6 (26%)
	2	9 (39%)
	>2	8 (40%)
Intracranial disease before ceritinib		
	Present	15 (65%)
	Absent	8 (35%)
Tabacco use history		
	Never	3 (3%)
	Previous or Current	20 (97%)

tients were not previously treated with an ALK TKI. Six patients were treatment-naïve. Fifteen patients presented intracranial disease before ceritinib and only 1 patient had received local treatment with whole brain radiotherapy before treatment initiation.

Treatment response

The objective response rate and disease control rates were 74% and 87%, respectively. At the end of July 2019, 1 patient remained progression-free and 5 patients continued treatment. Sixteen patients showed intracranial progression as the first disease progression site. Other extracranial progression sites included the pleura, liver, neck lymph nodes, and lung nodules. It was noteworthy that a majority (18 of 20) of the patients experienced their first disease progression involving a single organ only. The median PFS was 15 months; in all patients, the median OS was not reached by July 31, 2019 (Figure 1).

Treatment beyond progression

Twelve patients received ceritinib beyond progression, and the treatment duration after progression ranged from 2.7 to 65.5 months, with a median of 31.4 months. When comparing patients receiving ceritinib beyond progression to those who stopped ceritnib upon progression, we found that there were no differences regarding best response, PFS, or disease progression pattern. However, no one received local treatment at the time of progression in the group that stopped ceritinib, while 8 of 12 in the treatment beyond progression group had received local treatment. Among those patients that received local treatment, 6 received whole brain radiotherapy, 1 underwent brain surgery, and 1 received stereotactic ablative radiotherapy for 4 lung nodules. Four patients underwent a second local treatment for intracranial lesions during ceritinib treatment. For the 4 patients who did not receive local treatment at the time of progression, treatment duration after

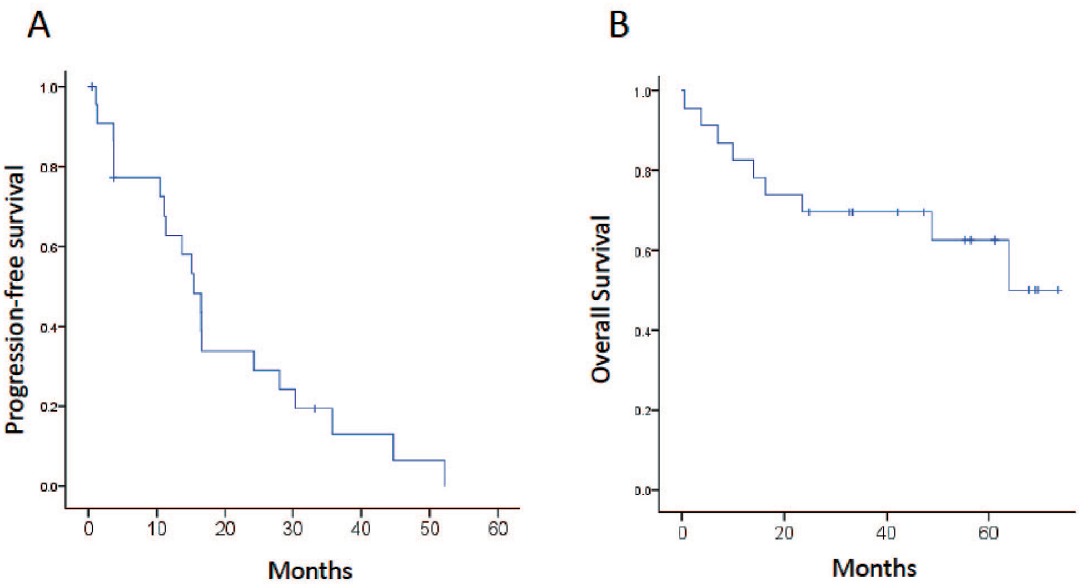

Fig. 1. Progression-free survival and overall survival of the 23 patients.

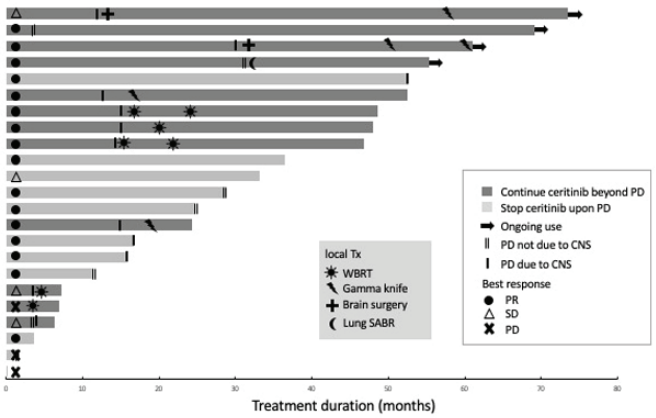

Fig. 2. Detailed course of treatment for the patients.

disease progression ranged from 24.3 months to 69 months. Three of the 4 had intracranial disease progression, and although they did not receive local treatment immediately, all eventually underwent radiotherapy for central nervous system (CNS) lesions 6 months later. Figure 2 summarizes the clinical course and local treatment of the patients.

Discussion

Ceritinib is a highly potent ALK TKI due to its better efficacy and superior cerebrospinal fluid penetration rate compared to crizotinib [5]. These pharmacological features have translated into clinical results, with ceritinib overcoming crizotinib resistance and demonstrating equal proportions of intracranial and non-intracranial disease progression patterns [4,6-7]. However, disease relapse was ultimately observed in these patients; several ceritinib resistance mechanisms have been reported, with G1202R the most common secondary ALK mutation [8]. Although the optimal next-line treatment is third-generation TKIs such as lorlatinib, concerns persist regarding the use of lorlatinib after ceritinib treatment. In patients presenting no secondary ALK mutations, the 4-month median PFS response rate was only 31% [9]. Moreover, tissue re-biopsy at the time of progression may not have been performed, particularly in those patients with intracranial progression. Besides lorlatinib, the platinum/pemetrexed combination is another therapeutic option. However, in a recently published retrospective study, Lin et al. reported that the response rate with chemotherapy was 29.7%, and the median PFS was 3.2 months after failing to respond to second-generation ALK TKIs [10]. Furthermore, although not as common as with epidermal growth factor receptor (EGFR) TKIs, the "disease flare phenomenon" was still reported after discontinuation of ALK TKIs [11]. This presented the treatment option of continuing TKI therapy beyond progression, with or without other therapies. In a 194-patient cohort, Ou *et al*. reported the clinical benefits of continuing crizotinib therapy [12]. In a poster presentation, Tan *et al*. retrospectively reported that patients who continued ceritinib in the ASCEND-1 and ASCEND -2 clinical trials had longer post-progression survival [13].

In patients receiving targeted therapy, continuation of the original systemic therapy with additional local treatment for oligoprogressive lesions has been widely discussed. Shukuya *et al*. first reported a study on 17 patients with EGFR mutations receiving local CNS treatment for isolated CNS oligoprogressive disease after establishing the clinical benefits of EGFR-TKI. They observed a median PFS of 80 days [14]. Subsequently, Yu *et al*, in a study on patients treated with non-CNS local therapy for oligoprogressive disease (<5 sites) while continuing EGFR-TKI treatment [15], reported an impressive median PFS of 10 months after local treatment. Further studies have also shown favorable disease control outcomes after both CNS and non-CNS local treatment [16]. Similar to those with EGFR mutations, patients with ALK mutations who respond to ALK TKI demonstrate an equal or even longer PFS. Hence, continuing ALK TKI therapy beyond disease progression seems to be an option in certain patient groups.

Indeed, Weickhardt *et al*. first reported a small group of ALK-positive patients that continued crizotinib after local therapy for oligoprogressive disease [17]. Subsequently, several groups have reported the flexibility and tolerability of continued crizotinib after local treatment for oligoprogressive disease [18]. Recently, Hong *et al*. presented their analysis of 33 Chinese patients who showed an initial benefit with crizotinib therapy, indicating that local therapy could be an independent predictor of post-initial PFS [19].

There were several limitations to our study. First, the small patient number may fail to comprehensively reflect the clinical course in this patient group. Second, as in previous clinical trials, different lines of ceritinib treatment may yield different response rates and median PFS, and our patient heterogeneity in the different ceritinib lines of treatment could have impacted the PFS results.

Conclusion

Our data indicate the high potency of ceritinib, comparable to previous clinical trials. Furthermore, we reported the feasibility and possible clinical benefits of continuing ceritinib treatment beyond progression, with or without added local therapy in selected patients.

References

1. Soda M, Choi YL, Enomoto M, *et al*. Identification of the transforming EML4-ALK fusion gene in non-small-cell lung cancer. Nature 2007; 448: 561-6.
2. Hallberg B, Palmer RH. The role of the ALK receptor in cancer biology. Ann Oncol 27; Suppl 3: iii4-iii15.
3. Solomon BJ, Kim DW, Wu YL, *et al*. Final overall survival analysis from a study comparing first-line crizotinib versus chemotherapy in ALK-mutation-positive non-small-cell lung cancer. J Clin Oncol 2018; 36: 2251-8.
4. Soria JC, Tan DSW, Chiari R, *et al*. First-line ceritinib versus platinum-based chemotherapy in advanced ALK-rearranged non-small-cell lung cancer (ASCEND-4): a randomised, open-label, phase 3 study. Lancet 2017; 389: 917-29.
5. Friboulet L, Li N, Katayama R, *et al*. The ALK inhibitor ceritinib overcomes crizotinib resistance in non-small cell lung cancer. Cancer Discov 2014; 4: 662-73.
6. Mok T, Spigel D, Felip E, *et al*. ASCEND-2: A single-arm, open-label, multicenter phase II study of ceritinib in adult patients (pts) with ALK-rearranged (ALK+) non-small cell lung cancer (NSCLC) previously treated with chemotherapy and crizotinib (CRZ). J Clin Oncol 2015; 33: 8059.
7. Shaw AT, Kim DW, Mehra R, *et al*. Ceritinib in ALK-rearranged non-small-cell lung cancer. N Engl J Med 2014; 370: 1189-97.
8. Lin JJ, Riely GJ, Shaw AT. Targeting ALK: precision

medicine takes on drug resistance. Cancer Discov 2017; 7: 137-55.

9. Shaw AT, Solomon BJ, Besse B, *et al*. ALK resistance mutations and efficacy of lorlatinib in advanced anaplastic lymphoma kinase-positive non-small-cell lung cancer. J Clin Oncol 2019; 37: 1370-9.
10. Lin JJ, Schoenfeld AJ, Zhu VW, *et al*. Efficacy of platinum/pemetrexed combination chemotherapy in ALK-positive NSCLC refractory to second-generation ALK inhibitors. J Thorac Oncol 2020; 15 (2): 258-265.
11. Pop O, Pirvu A, Toffart AC, *et al*. Disease flare after treatment discontinuation in a patient with EML4-ALK lung cancer and acquired resistance to crizotinib. J Thorac Oncol 2012; 7: e1-2.
12. Ou SH, Janne PA, Bartlett CH, *et al*. Clinical benefit of continuing ALK inhibition with crizotinib beyond initial disease progression in patients with advanced ALK-positive NSCLC. Ann Oncol 2014; 25: 415-22.
13. Tan D, Liu G, Kim DW, *et al*. 178P: continuation of ceritinib beyond disease progression is associated with prolonged post-progression survival (PPS) in ALK+ NSCLC. J Thorac Oncol 2016; 11: S134-S5.
14. Shukuya T, Takahashi T, Naito T, *et al*. Continuous EGFR-TKI administration following radiotherapy for non-small cell lung cancer patients with isolated CNS failure. Lung Cancer 2011; 74: 457-61.
15. Yu HA, Sima CS, Huang J, *et al*. Local therapy with continued EGFR tyrosine kinase inhibitor therapy as a treatment strategy in EGFR-mutant advanced lung cancers that have developed acquired resistance to EGFR tyrosine kinase inhibitors. J Thorac Oncol 2013; 8: 346-51.
16. Xu Q, Liu H, Meng S, *et al*. First-line continual EGFR-TKI plus local ablative therapy demonstrated survival benefit in EGFR-mutant NSCLC patients with oligoprogressive disease. J Cancer 2019; 10: 522-9.
17. Weickhardt AJ, Scheier B, Burke JM, *et al*. Local ablative therapy of oligoprogressive disease prolongs disease control by tyrosine kinase inhibitors in oncogene-addicted non-small-cell lung cancer. J Thorac Oncol 2012; 7: 1807-14.
18. Takeda M, Okamoto I, Nakagawa K. Clinical impact of continued crizotinib administration after isolated central nervous system progression in patients with lung cancer positive for ALK rearrangement. J Thorac Oncol 2013; 8: 654-7.
19. Hong X, Chen Q, Ding L, *et al*. Clinical benefit of continuing crizotinib therapy after initial disease progression in Chinese patients with advanced ALK-rearranged non-small-cell lung cancer. Oncotarget 2017; 8: 41631-40.

Risk Factors for 5-year Mortality in Patients Hospitalized with Congestive Heart Failure and Chronic Obstructive Pulmonary Disease

Chiung-Hung Lin[1], Jih-Kai Yeh[2], Ting-Yu Lin[1], Yu-Lun Lo[1], Po-Jui Chang[1]
Jia-Shiuan Ju[1], Tzu-Hsuan Chiu[1], Pi-Hung Tung[1], Shu-Min Lin[1,3]

Introduction: Heart failure (HF) is often comorbid with chronic obstructive pulmonary disease (COPD), which leads to more complex clinical management and a worse outcome. This study aimed to measure the prevalence of COPD in hospitalized HF patients using standard diagnostic criteria. The impact of COPD illness severity and medications on long-term outcomes of these patients were also investigated.

Methods: Patients hospitalized due to HF with a reduced ejection fraction (HFrEF) in a tertiary medical center were retrospectively recruited. The clinical outcomes, including length of hospital stay, mortality and readmission episodes, were examined and traced for 5 years. The risk factors for mortality were analyzed using multivariate analysis.

Results: The study retrospectively recruited 138 hospitalized patients with HFrEF. Sixty-eight of the patients were comorbid with COPD and 70 were not. A male predominance (88.2% vs 67.1%, p=0.003) and smoking history (87.9% vs 48.6%, p<0.001) were significant in the HF with COPD group. The left ventricular ejection fraction was decreased (mean 29.5% vs 32.6%, p=0.01) in HF patients with COPD compared to those without COPD. There was an increased length of hospital stay in the HF with COPD group compared to those without COPD (21.5±19.7 vs. 15.1±11.2, days; p=0.009). All-cause mortality and readmission were similar between the 2 groups. Multivariate analysis showed that the use of angiotensin receptor blockers (HR 0.375, 95% CI 0.150- 0.939, p=0.036) independently predicted 5-year survival.

Conclusion: The presence of COPD in HFrEF patients was associated with a prolonged length of hospital stay. Using guideline-recommended medications to treat patients with HFrEF combined with COPD plays an important role in their long-term outcome. ***(Thorac Med 2021; 36: 18-27)***

Key words: heart failure, COPD, mortality

[1]Department of Thoracic Medicine, Chang Gung Memorial Hospital, Chang Gung University, School of Medicine, Taipei, Taiwan
[2]Department of Cardiology, Linkou Chang Gung Memorial Hospital, Taiwan
[3]Department of Respiratory Therapy, Chang Gung Memorial Hospital, Chang Gung University, School of Medicine, Taipei, Taiwan
Address reprint requests to: Dr. Shu-Min Lin, Department of Thoracic Medicine,Chang Gung Memorial Hospital, 199 Tun-Hwa N. Rd., Taipei, Taiwan

Background

Heart failure (HF) is often comorbid with chronic obstructive pulmonary disease (COPD), which leads to more complex clinical management and a worse outcome [1]. In a 2014 study, 16% to 27% of patients with HF with a reduced ejection fraction (HFrEF) in the outpatient clinic and 10% to 31% of hospitalized patients had coexisting COPD [2]. HF and COPD share important risk factors, including smoking and systemic endothelial inflammation. There is also an increased frequency of a co-occurrence of coronary artery disease in patients with HF and COPD, due to similar mechanisms [3]. Other comorbidities that share part of the common mechanisms of HF and COPD also contribute to the disease prognosis.

The prevalence of COPD in HF is wide-ranging in epidemiological studies. This may be due to the use of clinical diagnoses of COPD and HF, without considering the criteria of the Global Initiative for Chronic Obstructive Lung Disease (GOLD) or reproducible echocardiographic parameters [4-5]. According to the GOLD guideline, the diagnosis of COPD includes smoking status and a pulmonary function test. The presence of obstructive impairment of lung function is mandatory in the diagnosis of COPD, but many epidemiological studies use only clinical diagnoses for COPD. The severity of airflow limitation in COPD patients also affects their clinical outcomes [6]. Therefore, there is a need to use objective criteria in the diagnosis of COPD in HFrEF patients. In addition, the impact of COPD illness severity on the clinical outcomes of patients with HF and COPD deserves further investigation.

The pharmacological therapies used for HF and COPD are important determinants of clinical outcomes. The guidelines suggest the use of angiotensin-converting enzyme inhibitors (ACEI), angiotensin receptor blockers (ARB), β-blockers (BB), and mineralocorticoid receptor antagonists (MRA) for the treatment of HFrEF patients [7]. The GOLD guideline recommends the use of inhaled bronchodilators and anti-inflammatory agents for the control of COPD [8]. However, the underuse of recommended medications is frequently found in clinical practice. For example, recent studies confirmed the safety of selective beta-1 blockers and inhaled bronchodilators for HF comorbid with COPD [4]. But clinical underuse of β-blockers due to a fear of bronchoconstriction was commonly observed, and this led to worsened outcomes [8]. The multiple comorbidities and complicated disease conditions of hospitalized HF and COPD patients may interfere with the use of medications. However, few studies have addressed the impact of these medications on the clinical outcomes of these patients.

This study aimed to measure the prevalence of COPD in hospitalized HF patients using standard diagnostic criteria. The impact of COPD illness severity and medications on the long-term outcomes of these patients were also investigated.

Materials and methods

Study population

The study retrospectively recruited patients hospitalized due to HFrEF from January 1, 2013 to December 31, 2015 in a tertiary medical center in Taiwan. HFrEF was defined as a left ventricular ejection fraction less than 40%, according to the 2013 American College of Cardiology Foundation (ACCF)/American Heart Association (AHA) guideline [7]. COPD

was defined according to the GOLD guideline as the presence of a post-bronchodilator forced expiratory volume in 1 second to forced vital capacity (FEV1/FVC) < 0.70 by spirometry, the presence of respiratory symptoms including dyspnea, chronic cough or sputum production, and smoking with at least a 10-pack-year history or a risk-factor exposure history [8]. The presence of a prior diagnosis of COPD was considered when the diagnosis with a compatible pulmonary function test was present as a part of the patients' past medical history.

The patients were divided into 2 groups based on the presence of COPD or not. The spirometry result, prior to admission or during hospitalization, was checked to determine the COPD diagnosis. Baseline characteristics including vital signs and laboratory data at admission, major underlying diseases, maintenance medications 3 months before admission, and clinical outcomes were recorded by reviewing the patient's electronic chart.

Clinical outcomes

Clinical outcomes, including length of hospital stay, mortality and readmission episodes, were examined and traced for 5 years. The contributions of COPD airflow limitation severity and comorbidities in clinical outcomes of the COPD group were also determined. The definitions of airflow limitation severity were based on the GOLD guideline [8]. In brief, mild, moderate, severe, and very severe obstruction were defined as an FEV1 >80%, FEV1 50% to 80%, FEV1 35% to 50%, and FEV1 <35% of predictive value, respectively.

Statistical analysis

All data were expressed as mean ± standard deviation (SD) or percentage. Comparison of continuous and nominal variables between 2 groups was performed using Student's t-test and the chi-square test, respectively. A p value of <0.05 using a 2-sided test was considered statistically significant. To determine the predictors for mortality, all variables with a p value <0.1 in univariate regression analysis were then entered into the forward logistic regression analysis model to identify independent predictive factors for mortality outcome. Odds ratios (OR) and their 95% confidence intervals (CI) were computed to clarify the impact of several potentially independent prognostic factors. The proportions of free-from-readmission and mortality were plotted using the Kaplan-Meier curve, and significance was examined with the log-rank test. A p value <0.05 using a 2-sided test was considered statistically significant. All statistical analyses were performed using SPSS software, version 20.0 (SPSS, Inc., Chicago, IL).

Ethics Approval and Consent to Participate

The Chang Gung Medical Foundation Institutional Review Board (201900648B0) approved the study and waived the requirement for informed consent, due to the retrospective nature of the study.

Results

Characteristics of the study population

In all, 138 consecutively hospitalized patients with HFrEF were recruited for this study; 68 of them were comorbid with COPD and 70 of them were not. Baseline patient characteristics are listed in Table 1. Both male predominance (88.2% vs 67.1%, p=0.003) and smoking history (87.9% vs 48.6%, p<0.001) were significant in the HF with COPD group. The left ven-

Table 1. Baseline Patient Characteristics (n=138)

	HF with COPD (n=68)	HF without COPD (n=70)	*P* value
Age (years)	73.3 ± 10.4	70.6 ± 15.6	0.242
Male (n, %)	60 (88.2%)	47 (67.1%)	0.003
Smoking (n, %)	58 (87.9%)	35 (48.6%)	<0.001
BMI at discharge (kg/m^2)	22.7 ± 3.5	23.3 ± 3.6	0.297
Underlying diseases, (n, %)			
Coronary artery disease	34 (50.0%)	39 (55.7%)	0.501
Diabetes mellitus	24 (35.3%)	29 (41.4%)	0.459
Dyslipidemia	48 (70.6%)	53 (75.7%)	0.497
Hypertension	63 (92.6%)	63 (90.0%)	0.581
Chronic kidney disease	26 (38.2%)	27 (38.6%)	0.968
Atrial fibrillation	22 (32.4%)	16 (22.9%)	0.212
Stroke	7 (10.3%)	11 (15.7%)	0.345
Vital signs and laboratory tests, (mean ± ds)			
SBP (mmHg)	124.7 ± 24.0	124.1 ± 20.0	0.881
DBP (mmHg)	74.2 ± 14.4	73.8 ± 12.9	0.852
HR (bpm)	86.2 ± 18.5	85.5 ± 17.1	0.835
LVEF, %	29.5 ± 7.8	32.6 ± 6.1	0.010
Hemoglobin (g/dl)	12.8 ± 2.2	12.2 ± 2.3	0.132
Potassium (mmol/l)	4.2 ± 0.4	4.1 ± 0.5	0.737
Sodium (mmol/l)	138.6 ± 4.0	139.1 ± 4.0	0.417
Glucose (mmol/l)	138.0 ± 49.0	135.5 ± 44.0	0.754
Creatinine (μmol/l)	1.6 ± 1.4	1.9 ± 2.1	0.314
Baseline medications, (n, %)			
Selective beta-1 blocker	14 (20.6%)	13 (18.6%)	0.765
Nonselective beta blocker	12 (17.6%)	18 (25.7%)	0.251
ACEI	2 (2.9%)	9 (12.9%)	0.032
ARB	37 (54.4%)	35 (50.0%)	0.604
MRA	28 (41.2%)	20 (28.6%)	0.120
SABA	10 (15.4%)	0	.
LAMA	24 (36.9%)	0	.
LABA	30 (46.2%)	0	.
ICS	24 (36.9%)	0	.
OCS	8 (12.3%)	0	.

Data were expressed as mean ± SD

Acronyms:

HF: heart failure; COPD: chronic obstructive pulmonary disease; BMI: body mass index; SBP: systolic blood pressure; DBP: diastolic blood pressure; HR: heart rate; ACEI: angiotensin converting enzyme inhibitor; ARB: angiotensin receptor blocker; MRA: mineralocorticoid receptor antagonist; SABA: short-acting β agonist; LABA: long-acting β agonist; LAMA: long-acting muscarinic antagonist; ICS: inhaled corticosteroid; OCS: oral corticosteroid; LVEF: left ventricular ejection fraction

tricular ejection fraction (LVEF) was decreased (mean 29.5% vs 32.6%, p=0.01) among HF patients with COPD compared to those without.

Clinical Outcomes

A comparison of clinical outcomes between HFrEF patients with and without COPD is shown in Table 2. There was a significantly increased length of hospital stay in the HF with COPD group compared to those without (21.5 ± 19.7 vs. 15.1 ± 11.2 days; p=0.009). The mean survival times and the time to first readmission were similar between the 2 groups, as were the all-cause mortality and readmission rates.

A comparison of clinical outcomes of HFrEF with COPD patients according to COPD airflow limitation severity is shown in Table 3. The study stratified the subjects into 2 groups: mild-to-moderate and severe-to-very-severe airflow limitation. However, there was no significant difference in mortality and readmission rates between the 2 groups.

Analysis of factors associated with mortality in patients with HF and COPD

We employed univariate and multivariate logistic regression analysis to determine the independent effect of clinical variables (Table 4). In univariate analysis, the use of ARB and inhaled corticosteroids was primarily selected with a cutoff p value of 0.1. In multivariate analysis, only the use of ARB (HR 0.375, 95% CI 0.150- 0.939, p=0.036) independently predicted 5-year survival.

Table 2. Comparison of Clinical Outcomes between Heart Failure Patients with and without COPD

	With COPD (n=68)	Without COPD (=70)	*P* value
Length of hospital stay, days	21.5 ± 19.7	15.1 ± 11.2	0.009
Survival duration, days	1330.2 ± 661.9	1451.5 ± 649.4	0.279
Duration to 1st admission, days	490.1 ± 642.7	532.1 ± 700.1	0.715
All-cause mortality (n, %)			
In-hospital	2 (3.0%)	2 (2.8%)	0.930
30-day	5 (7.4%)	3 (4.3%)	0.343
90-day	5 (7.4%)	5 (7.1%)	0.609
1-year	12 (17.6%)	9 (12.9%)	0.434
5-year	22 (32.4%)	18 (25.7%)	0.390
All-cause readmission (n, %)			
30-day	12 (17.6%)	7 (10.0%)	0.192
90-day	25 (36.8%)	18 (25.7%)	0.161
1-year	41 (60.3%)	42 (60.0%)	0.972
5-year	55 (80.9%)	53 (75.7%)	0.462

Data were expressed as mean ± SD

Acronym: COPD: chronic obstructive pulmonary disease

Table 3. Clinical Outcomes Stratified According to COPD Severity

	Mild to moderate COPD (n=40)	Severe to very severe COPD (n=28)	*P* value
All-cause mortality			
In-hospital	2 (5.0%)	0	0.342
30-day	5 (12.5%)	0	0.063
90-day	5 (12.5%)	0	0.063
1-year	10 (25.0%)	2 (7.1%)	0.054
5-year	15 (37.5%)	7 (25.0%)	0.278
All-cause readmission			
30-day	7 (17.5%)	5 (17.9%)	0.607
90-day	17 (42.5%)	8 (28.6%)	0.241
1-year	28 (68.3%)	13 (46.4%)	0.051
5-year	34 (85.0%)	21 (75.0%)	0.302

Acronym: COPD: chronic obstructive pulmonary disease

There was no difference in mortality rate and readmission rate between the HF with COPD and HF without COPD group using Kaplan-Meier analysis (Figure 1A & 1B). The use of ARB in the HF with COPD group showed a survival benefit (log rank test, p=0.012, HR: 0.336, 95% CI: 0.144- 0.784, Figure 1C), but no difference in readmission rate (Figure 1D).

Discussion

COPD is a common comorbidity of hospitalized HFrEF patients. The presence of COPD is associated with a prolonged length of hospital stay. However, the mortality and readmission rates were unaffected by a comorbidity of COPD. In the HFrEF with COPD group, the use of ARB was an independent predictor for better survival, while COPD airflow limitation severity did not affect the mortality and readmission rates.

Compatible with previous studies [10], our results showed that HFrEF patients with COPD have a longer length of hospital stay than those without COPD. Patients with HFrEF combined with COPD had depressed LVEF and a higher rate of smoking than those without COPD. In addition, COPD patients were defined as having FEV_1/FVC <0.70 in spirometry. Thus, lung functioning in COPD patients was worse than in patients without COPD. Taken together, the higher illness severity rate in patients with HFrEF and COPD may contribute to the longer hospital stay for these patients than for those without COPD. Due to our recruitment of hospitalized patients with HFrEF, high readmission rates and 5-yr mortality rates were found in both groups. The first-year readmission rates were as high as 60% and 5-yr mortality was at least 25% in both groups. The similar 5-yr mortality and readmission rates in this study may be due to the high baseline severity of HF in the study population. In another study, multivariant analysis also showed that the presence of a COPD comorbidity in HF patients did not increase mortality rates [11].

Table 4. Univariate and Multivariate Analysis for All-cause Mortality in the HF + COPD Group

	Univariate analysis			Multivariate analysis		
	HR	95% CI	*P*-value	HR	95% CI	*P*-value
Age	1.026	(0.981- 1.073)	0.269			
Gender (male vs female)	1.381	(0.323- 5.908)	0.664			
COPD severity (severe to very severe vs mild to moderate)	0.564	(0.230- 1.385)	0.212			
Hypertension (yes vs no)	1.919	(0.258- 14.274)	0.524			
DM (yes vs no)	1.118	(0.469- 2.665)	0.802			
CAD (yes vs no)	0.803	(0.525- 1.229)	0.312			
Dyslipidemia (yes vs no)	1.488	(0.549- 4.034)	0.435			
CKD (yes vs no)	1.049	(0.448- 2.454)	0.912			
Afib (yes vs no)	0.976	(0.398- 2.393)	0.957			
Stroke (yes vs no)	2.157	(0.728- 6.394)	0.166			
EF	0.990	(0.939- 1.045)	0.725			
β-1 blocker (yes vs no)	1.241	(0.457- 3.365)	0.672			
Nonselective β blocker (yes vs no)	0.722	(0.214- 2.441)	0.600			
ACEI (yes vs no)	2.548	(0.342- 18.969)	0.361			
ARB (yes vs no)	0.333	(0.136- 0.817)	0.016*	0.375	(0.150- 0.939)	0.036*
MRA (yes vs no)	0.758	(0.318- 1.810)	0.533			
SABA (yes vs no)	1.077	(0.364- 3.182)	0.894			
LABA (yes vs no)	0.601	(0.260- 1.393)	0.235			
LAMA (yes vs no)	0.971	(0.407- 2.316)	0.948			
ICS (yes vs no)	2.124	(0.920- 4.904)	0.078	2.299	(0.223- 23.560)	0.074
OCS (yes vs no)	1.950	(0.659- 5.775)	0.228			

Acronyms:

COPD: chronic obstructive pulmonary disease; DM: diabetes mellitus; CAD: coronary artery disease; CKD: chronic kidney disease; Afib: atrial fibrillation; EF: ejection fraction; ACEI: angiotensin converting enzyme inhibitor; ARB: angiotensin receptor blocker; MRA: mineralocorticoid receptor antagonist; SABA: short-acting β agonist; LABA: long-acting β agonist; LAMA: long-acting muscarinic antagonist; ICS: inhaled corticosteroid; OCS: oral corticosteroid

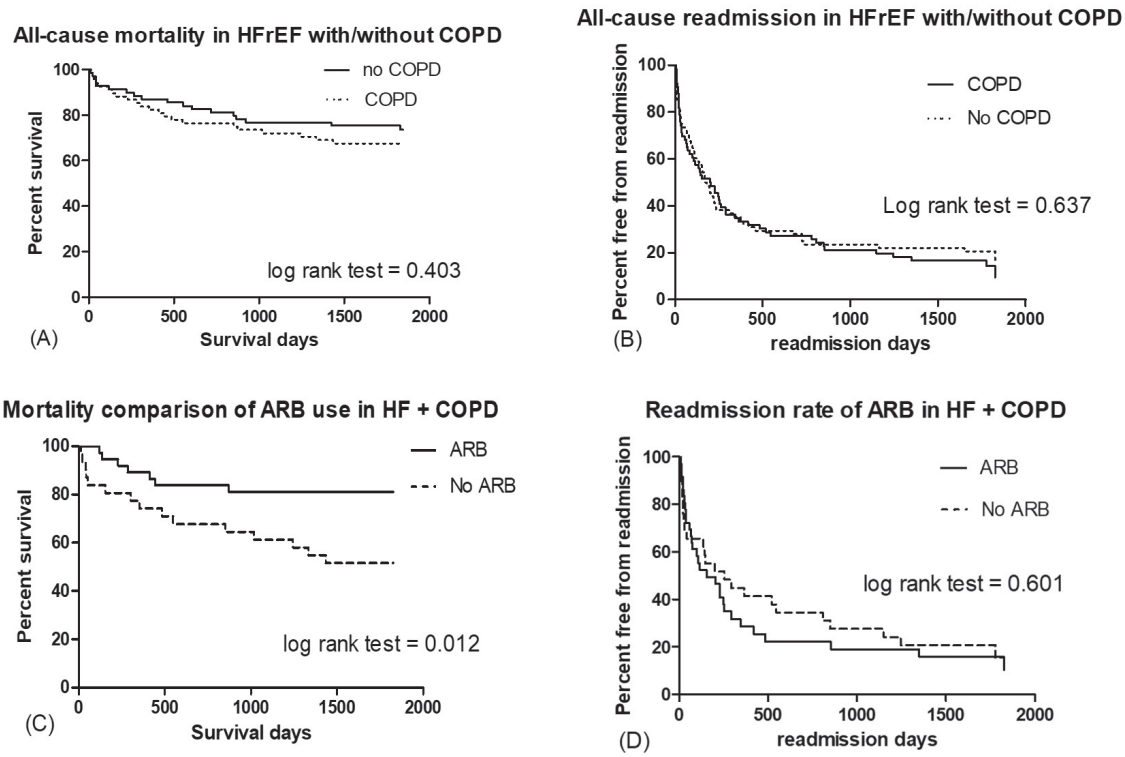

Fig. 1. Proportions of Free-from-Readmission and Mortality in Patients Traced Using the Kaplan-Meier Method
(A). The 5-yr all-cause mortality rate in patients with HFrEF. The dashed line represents patients with HFrEF and COPD; the continuous line represents patients with HFrEF without COPD. (B). The 5-yr all-free-from-readmission rate of patients with HFrEF. The dashed line represents patients with HFrEF and COPD; the continuous line represents patients with HFrEF without COPD. (C). The 5-yr all-cause mortality in patients with HFrEF and COPD. The dashed line represents patients that did not receive angiotensin receptor blocker (ARB) treatment; the continuous line represents patients that did receive ARB treatment. (D). The 5-yr free-from-readmission rate in patients with HFrEF and COPD. The dashed line represents patients that did not receive ARB treatment; the continuous line represents patients that did receive ARB treatment

The present study found that the degree of airflow limitation, as indicated by the FEV1 value, was not predictive for 5-yr readmission and mortality rates. Plesner LL *et al*. reported no association between all-cause mortality and the degree of airflow limitation in HF with COPD patients [12]. However, another study reported an increase in mortality with increases in the severity of airflow limitation in a comparison of patients with and without COPD. This discrepancy may be due to the use of different inclusion criteria in these studies. In the above study, there was no LVEF data [7]. So, the study population contained both HFrEF and HF with a preserved ejection fraction (HFpEF), which is different from our study population. In fact, the updated GOLD guideline stratifies the severity of COPD using the symptom score and incidence of acute exacerbation rather than the degree of airflow limitation. Besides, the fluid overload in HF may interfere with the airflow limitation. Emerging evidence suggests that an overestimation of COPD severity based on FEV_1 may happen in HF with COPD patients. FEV_1 usually decreases to an extent equal to FVC in HF patients. FEV_1 may be low despite

no or little airway limitation, leading to error in interpretation and result [13]. Therefore, the status of lung function impairment in patients with HFrEF and COPD may not be a good indicator of clinical outcomes.

Adequate medical therapy in accordance with the guidelines is crucial to the clinical outcomes of patients with HFrEF comorbid with COPD. The ACCF/AHA guideline for the management of HF suggests the use of ARB in HFrEF patients to reduce mortality and hospitalization [14]. The use of ARB in COPD patients has been reported to be associated with a decreased mortality rate [15] and a lower rate of pneumonia [16]. In our study, multivariate analysis found that the use of ARB had an independent, beneficial effect on the survival of patients with coexisting HFrEF and COPD. Although ARB is the recommended medication in the guidelines, these medications are frequently not prescribed in clinical practice. The underuse of ARB is associated with an increased risk of death. The common reasons for not prescribing ARB are impaired renal function, hyperkalemia, low systolic blood pressure, cancer history and old age. Bertero E *et al*. reported that worsening renal function and low blood pressure do not impact ARB user outcomes. Reducing the medication dosage is needed in advanced chronic kidney disease. Careful up-titration of ARB is recommended in the presence of hypotension [17]. Considering its benefits, it is important to use ARB in patients with HFrEF and COPD.

In univariate analysis, the use ARB, but not ACEI, had a survival benefit for patients with HFrEF and COPD. To the best of our knowledge, there is no study directly comparing the effects of ACEI and ARB treatment on patients with HFrEF coexisting with COPD. However, a recent study reported that the use of ARB treatment for COPD patients was associated with decreased incidences of severe exacerbations, pneumonia, and mortality compared to the use of ACEI. The probable mechanism may be related to the additional anti-inflammatory effect of ARB [16]. An animal study also found that ARB had protective effects on bleomycin-induced pulmonary injuries [18]. In addition, the low incidence of ACEI use in our study population may have biased a determination of the effects of ACEI on clinical outcomes. Further studies comparing the effects of ACEI and ARB use, respectively, in patients with HFrEF combined with COPD are needed to elucidate the differences between these 2 medications.

A major limitation of the present study is its retrospective nature, which may have led to a bias in the selection of study subjects. In addition, the sample size in this study was small; therefore, the results should be interpreted with caution. Lastly, the study recruited hospitalized HFrEF patients whose illness severity may have been higher than that of patients in outpatient clinics. The clinical outcomes may have been affected by the disease severity. A prospective study with a larger sample size is warranted to further confirm the clinical outcomes of patients HFrEF and COPD.

In conclusion, COPD is a common comorbidity of patients with HFrEF. The presence of COPD in HFrEF patients was associated with a prolonged length of hospital stay. Treatment of patients with HFrEF and COPD with guideline-recommended medications will play an important role in their long-term outcomes.

Funding

This project was supported by the Ministry of Science and Technology of Taiwan, R.O.C.

(MOST 105-2314-B-182A-146-MY2) and research grants from Chang Gung Memorial Hospital, Taiwan (CIRPG3H0051).

References

1. Mentz RJ, Kelly JP, von Lueder TG, *et al*. Noncardiac comorbidities in heart failure with reduced versus preserved ejection fraction. J Am Coll Cardiol. 2014; 64(21): 2281-93.
2. Triposkiadis F, Giamouzis G, Parissis J, *et al*. Reframing the association and significance of co-morbidities in heart failure. Eur J Heart Fail. 2016; 18(7): 744-58.
3. Smith MC, Wrobel JP. Epidemiology and clinical impact of major comorbidities in patients with COPD. Int J Chron Obstruct Pulmon Dis. 2014; 9: 871-88.
4. Guder G, Stork S. COPD and heart failure: differential diagnosis and comorbidity. J Card Fail. 2019; 44(6): 502-8.
5. De Miguel Diez J, Chancafe Morgan J, Jimenez Garcia R. The association between COPD and heart failure risk: a review. Int J Chron Obstruct Pulmon Dis. 2013; 8: 305-12.
6. Lawson CA, Mamas MA, Jones PW, *et al*. Association of medication intensity and stages of airflow limitation with the risk of hospitalization or death in patients with heart failure and chronic obstructive pulmonary disease. JAMA Netw Open. 2018; 1(8): e185489.
7. Yancy CW, Jessup M, Bozkurt B, *et al*. 2013 ACCF/AHA guideline for the management of heart failure: a report of the American College of Cardiology Foundation/American Heart Association Task Force on Practice Guidelines. J Am Coll Cardiol. 2013; 62(16): e147-239.
8. Global Initiative for Chronic Obstructive Lung Disease. 2020 Global strategy for prevention, diagnosis and management of COPD. 2019.
9. Lipworth B, Skinner D, Devereux G, *et al*. Underuse of β-blockers in heart failure and chronic obstructive pulmonary disease. Heart. 2016; 102(23): 1934.
10. Axson EL, Ragutheeswaran K, Sundaram V, *et al*. Hospitalisation and mortality in patients with comorbid COPD and heart failure: A systematic review and meta-analysis. Respir Res. 2020; 21(1): 54.
11. Staszewsky L, Wong M, Masson S, *et al*. Clinical, neurohormonal, and inflammatory markers and overall prognostic role of chronic obstructive pulmonary disease in patients with heart failure: data from the Val-HeFT heart failure trial. J Card Fail. 2007; 13(10): 797-804.
12. Plesner LL, Dalsgaard M, Schou M, *et al*. The prognostic significance of lung function in stable heart failure outpatients. Clin Cardiol. 2017; 40(11): 1145-51.
13. Guder G, Rutten FH, Brenner S, *et al*. The impact of heart failure on the classification of COPD severity. J Card Fail. 2012; 18(8):637- 44.
14. Yancy CW, Jessup M, Bozkurt B, *et al*. 2017 ACC/AHA/HFSA focused update of the 2013 ACC/AHA guideline for the management of heart failure. JACC. 2017; 70(6): 776-803.
15. Paulin P, Maritano Furcada J, Ungaro CM, *et al*. Effect of angiotensin 2 receptor blockers on chronic obstructive lung disease mortality: A retrospective cohort study. Pulm Pharmacol Ther. 2017; 44: 78-82.
16. Lai CC, Wang YH, Wang CY, *et al*. Comparative effects of angiotensin-converting enzyme inhibitors and angiotensin II receptor blockers on the risk of pneumonia and severe exacerbations in patients with COPD. Int J Chron Obstruct Pulmon Dis. 2018; 13: 867-74.
17. Bertero E, Miceli R, Lorenzoni A, *et al*. Causes and impact on survival of underuse of angiotensin-converting enzyme inhibitors and angiotensin II receptor blockers in heart failure. Intern Emerg Med. 2019; 14(7): 1083-90.
18. Mancini GB, Khalil N. Angiotensin II type 1 receptor blocker inhibits pulmonary injury. Clin Invest Med. 2005; 28(3): 118-26.

Performance of Xpert MTB/RIF Assay for Detection of Mycobacterium Tuberculosis in Respiratory Specimens and Its Effect on Reducing TB Diagnosis Delay: A Single Center Experience

Chia-Jung Liu[1], Meng-Rui Lee[1], Pei-Lan Shao[2], Jann-Yuan Wang[3], Jen-Chung Ko[1]

Background: Xpert MTB/RIF (GeneXpert MTB/RIF) assay is a point-of-care nucleic acid amplification test (NAAT) endorsed by the World Health Organization for rapid detection of *Mycobacterium tuberculosis* (MTB) from respiratory specimens. Studies regarding its performance and impact on tuberculosis (TB) diagnosis in Taiwan remain limited.

Methods: This was a single-center study conducted in northern Taiwan. Patients with suspected pulmonary TB and who had respiratory specimens examined by Xpert MTB/RIF from January 2016 to July 2020 were recruited. We evaluated the performance of Xpert MTB/RIF using the culture method as a reference. The results of conventional MTB NAAT (Cobas TaqMan) were also recorded and compared.

Results: A total of 102 patients were recruited. Among them, 23 were positive using MTB culture and 20 were positive using acid-fast stain. The sensitivity and specificity of Xpert MTB/RIF were 91.3% (21/23) and 100% (79/79), respectively. Cobas TaqMan was also performed for 51 patients, with a sensitivity and specificity of 66.7% (8/12) and 100% (39/39), respectively. Use of Xpert MTB/RIF reduced TB diagnosis delay by 2 days compared to traditional stain and culture methods. Among the 8 patients with smear-negative TB, the median time to MTB culture positivity was 26.5 days (total=219 days).

Conclusion: Xpert MTB/RIF is a sensitive and specific point-of-care diagnosis kit for MTB detection in respiratory specimens, and helps reduce TB diagnosis delay. ***(Thorac Med 2021; 36: 28-34)***

Key words: diagnosis delay, *Mycobacterium tuberculosis*, nucleic acid amplification test, real-time polymerase chain reaction, Xpert MTB/RIF

[1]Department of Internal Medicine, National Taiwan University Hospital, Hsin-Chu Branch, Taiwan
[2]Department of Laboratory Medicine, National Taiwan University Hospital, Hsin-Chu Branch, Taiwan
[3]Department of Internal Medicine, National Taiwan University Hospital, Taipei, Taiwan, ROC
Address reprint requests to: Dr. Meng-Rui Lee, Department of Internal Medicine, National Taiwan University Hospital, Hsinchu Branch, No. 25, Ln. 442, Sec. 1, Jingguo Road, Hsinchu 300, Taiwan

Introduction

Tuberculosis (TB) is still a very significant infectious disease, and remains among the top 10 causes of death globally [1]. Immediate diagnosis and detection is an irreplaceable component of adequate pulmonary TB control [2]. Laboratory identification of Mycobacterium tuberculosis (MTB) traditionally relies on acid-fast stain and culture methods. Not until recently have newer molecular techniques for MTB detection been available. Among the various molecular diagnostic techniques, the GeneXpert MTB/RIF (Xpert MTB/RIF) assay (Cepheid, CA, USA) is undoubtedly one of the most widely used commercial kits [3]. The Xpert MTB/RIF assay is a nucleic-acid amplification test (NAAT) designed for detecting MTB complex deoxyribonucleic acid (DNA) in sputum or concentrated sputum sediments. The Xpert MTB/RIF assay is also able to detect rifampicin resistance-associated mutations of the *rpoB* gene [4]. Furthermore, Xpert MTB/RIF is designed as a portable, automatic sample processing system, having a short turnaround time of 2-3 hours [5]. Xpert MTB/RIF is, therefore, endorsed by the World Health Organization as a point-of-care test for TB, scheduled to be used in TB endemic and resource-limited areas [6].

The performance of the Xpert MTB/RIF assay has been reported in various studies [7]. In a multi-nation verification study, the Xpert MTB/RIF assay identified 551 of 561 smear-positive TB specimens (98.2%) and 124 of 171 smear-negative TB specimens (72.5%) using culture as the reference standard [7]. In a meta-analysis that included 27 studies and 9557 participants, pooled sensitivity was 89% and pooled specificity was 99% when Xpert MTB/RIF was used in place of smear microscopy. Following initially negative smear microscopy results, pooled Xpert test sensitivity was 67% and pooled specificity was 99% [8]. The cost-effectiveness of Xpert is also very promising. In a study evaluating Xpert cost-effectiveness in African countries using a calibrated dynamic mathematical model, Xpert offered reasonable value for its cost based on traditional benchmarks for cost-effectiveness [9].

The effectiveness of Xpert in Taiwan, however, has not been widely studied. Furthermore, no studies have discussed the benefit and effectiveness of reducing TB diagnosis delay with the use of Xpert. Therefore, we conducted this study in order to investigate the performance of Xpert in a regional hospital in Taiwan, which is an intermediate TB burden country [10]. We also evaluated the effect of reducing TB diagnosis delay using the Xpert test.

Methods

Participant recruitment, specimen collection and processing

This study was conducted at National Taiwan University Hospital (NTUH), Hsin-Chu Branch, a 600-bed regional hospital located in northern Taiwan. Respiratory specimens of patients with suspected pulmonary TB were collected for acid-fast smear and mycobacterial culture. The results of the Xpert test were compared with those obtained from conventional culture methods. Only those with concomitant Xpert, acid-fast stain and culture results were included in our study and analysis. Cobas TaqMan MTB assay is also available in our institute as another TB real-time polymerase chain reaction kit [11]. Therefore, the Cobas TaqMan MTB results were also recorded and compared with the Xpert results. All patients included in

this study underwent only one Xpert MTB/RIF assay. If multiple Cobas TaqMan tests were being ordered, the overall Cobas TaqMan result was interpreted as positive if any one of the Cobas TaqMan tests was positive, and as negative if all Cobas TaqMan tests were negative. The study was approved by the Institutional Review Board of National Taiwan University Hospital, Hsin-Chu Branch, and patient consent was waved because this study did not add additional risk to the patients.

All specimens for acid-fast bacilli staining and mycobacterial culture were processed and pretreated as previously described [11-12]. Acid-fast bacilli smears of the processed specimens were stained with auramine-rhodamine fluorochrome and examined using standard procedures [11-12]. For mycobacterial culture, we used Lowenstein–Jensen medium (solid culture) and the Mycobacterium Growth Indicator Tube (MGIT, liquid culture) with the BACTEC™ MGIT™ automated mycobacterial detection system [13].

Definition of TB diagnosis delay reduction

While hospitals may differ in the timeliness of processing respiratory specimens and generating acid-fast results, we assumed that Xpert MTB/RIF and acid-fast staining could be processed and reported the same day. We also assumed that a positive acid-fast stain would at least alert physicians to the possibility of TB and thereby avoid a diagnosis delay. TB diagnosis delay reduction, therefore, was defined as the time to culture positivity among smear-negative TB in this study. TB diagnosis delay will be calculated as the sum of time to culture positivity among all smear-negative TB patients..

Xpert MTB/RIF

Xpert MTB/RIF assay tests were conducted per the manufacturer's instructions and as previously reported [14]. In short, a 500-µl sputum sample was added to a sample reagent at a 1:3 ratio in an Xpert MTB/RIF 15-ml centrifuge tube and incubated at room temperature for 15 minutes. Within every 5 minutes during incubation, the samples were mixed by inverting the tubes gently 2 times. Then, 2.0 ml of liquefied sample was transferred to an Xpert MTB/RIF cartridge (G4 version) and loaded into the Xpert MTB/RIF machine. Results were available within 2 hours of sample loading.

Cobas TaqMan MTB assay

The Cobas TaqMan MTB assay was conducted according to the manufacturer's instructions and as previously described [11]. In brief, 100-µl aliquots of the decontaminated respiratory specimens were mixed with 500 µl of specimen wash solution and then centrifuged. The supernatant was discarded and the pellet was then lysed. The samples were processed using the Cobas TaqMan 48 Analyzer (Roche Diagnostics, Basel, Switzerland).

Statistical analysis

Sensitivity, specificity and accuracy analyses were performed to evaluate the performance of Xpert MTB/RIF for diagnosing pulmonary TB. Sensitivity was defined as the probability of pulmonary TB patients having positive Xpert MTB/RIF results. Specificity was defined as the probability of patients without pulmonary TB having negative Xpert MTB/RIF results. Accuracy was defined as the proportion of true positives and true negatives among all evaluated cases [15]. The sensitivity and accuracy rates of Xpert MTB/RIF and Cobas TaqMan were compared using Fisher's exact test. All p values

Table 1. Diagnostic Performance of the Xpert MTB/RIF assay, Stratified by Acid-fast Smear Results

Results of acid-fast smear (no. of specimens)	Results of Xpert MTB/RIF (no. of specimens)	No. of specimens		Sensitivity (%)	Specificity (%)
		Culture-positive for MTB	Culture-negative for MTB		
Positive (20)	Positive (13)	13	0	92.9	100
	Negative (7)	1	6		
Negative (82)	Positive (8)	8	0	88.9	100
	Negative (74)	1	73		
All (102)		23	79	91.3	100

were 2-sided and statistical significance was set at $p < 0.05$.

Results

During the study period (January 2016 to July 2020), a total of 10,516 patients had respiratory specimens examined in our institute using acid-fast stain and mycobacterial culture. Among them, 430 culture-positive pulmonary TB patients were diagnosed. A total of 102 patients were included for analysis in this study. Of the 102 patients, 23 were diagnosed with pulmonary TB with a positive MTB culture, and 20 (19.6%) were smear-positive using acid-fast bacilli. Using the culture method as the reference, the sensitivity and specificity of Xpert MTB/RIF for diagnosing pulmonary TB were 91.3% (21/23) and 100% (79/79), respectively. In patients with a positive acid-fast smear (n=20), the sensitivity and specificity of Xpert MTB/RIF were 92.9 (13/14) and 100% (6/6), respectively. In those with a negative acid-fast smear (n=82), the sensitivity and specificity of Xpert MTB/RIF were 88.9% (8/9) and 100% (73/73), respectively (Table 1).

Effect of Xpert on reducing TB diagnosis delay

For the 8 patients with smear-negative, culture-positive pulmonary TB, the median duration of diagnosis delay was 26.5 days based on culture (total, 219 days, range, 14 to 36 days) and 1 day based on Xpert MTB/RIF. For the total 102 tests, TB diagnosis delay was reduced by 219 days, meaning that the use of every single Xpert MTB/RIF test contributed to a 2-day reduction in TB diagnosis delay.

Comparison of Xpert MTB/RIF and Cobas TaqMan

Cobas TaqMan was also performed for 51 of the 102 patients. The sensitivity and specificity of the Cobas TaqMan kit were 66.7% (8/12) and 100% (39/39), respectively. The Xpert MTB/RIF and Cobas TaqMan results were concordant with culture in 46 (90.2%) patients. In 4 TB patients, Xpert MTB/RIF was positive while Cobas TaqMan was negative. In 1 TB patient, Xpert MTB/RIF was negative and Cobas TaqMan was positive.

The accuracy of Xpert MTB/RIF and Cobas TaqMan using the culture method as a reference was 98.1% (50/51) and 92.2% (47/51), respectively (Fisher's exact test p=0.922). The sensitivity of Xpert MTB/RIF and Cobas TaqMan was 92.7% (11/12) and 66.7% (8/12), respectively (Fisher's exact test p=0.667).

Discussion

In our study, the performance of Xpert MTB/RIF in diagnosing pulmonary TB was good, compared to traditional culture methods. The sensitivity and specificity of Xpert MTB/RIF were 91.3% and 100%, respectively. In the setting of our institute, each Xpert MTB/RIF test may help reduce TB treatment delay by 2 days. The performance of Xpert MTB/RIF was not inferior to that of Cobas TaqMan, though the case number was limited.

Xpert MTB/RIF is a point-of-care TB diagnosis kit that is increasingly used worldwide [6]. In a recent meta-analysis including 70 studies and 37,237 unselected participants, Xpert MTB/RIF had a pooled sensitivity and specificity of 85% (95% credible interval (CrI)): 82% to 88%) and 98% (95% CrI: 97% to 98%), respectively [6]. In our search of current literature, we found 1 journal article and 2 conference posters regarding the performance of Xpert MTB/RIF in diagnosing TB in Taiwan [14,16-17]. When combining the results of the 3 published reports and our current study, the overall sensitivity and specificity of Xpert MTB/RIF were 77.1% and 92.0% for a total of 4518 respiratory specimens. Two studies (the study by Chiang et al. and the present study) reported acid-fast stain results [14]. The sensitivity and specificity of smear-positive specimens (n=1115) were 94.5% and 64.2%, respectively, and that for smear-negative specimens (n=1650) were 40% and 95.5%, respectively (Table 2).

Comparing older and newer methods of TB NAATs has always been an area of interest. Cobas TaqMan is one of the most frequently used rapid molecular diagnostic tests, and has been compared to Xpert MTB/RIF in several studies. In a study that included 320 consecutive respiratory specimens, the overall sensitivities of the Cobas and Xpert assays were 71.4% and 67.9%, respectively, with TB culture as a reference method [18]. In another study including

Table 2. Performance of the Xpert MTB/RIF Assay for Detection of *M. Tuberculosis* in Respiratory Specimens in Taiwan in the Literature.

Study	No. of specimens	Sensitivity (%)	Specificity (%)	Acid-fast smear-positive specimens			Acid-fast smear-negative specimens		
				No. of specimens	Sensitivity (%)	Specificity (%)	No. of specimens	Sensitivity (%)	Specificity (%)
Chiang *et al.* (2018) [14]	2663	73.9	86.0	1095	94.5	63.8	1568	38.7	95.3
Chou *et al.* (2018) [17]*	1641	90.1	98.1	NA	NA	NA	NA	NA	NA
Hsu *et al.* (2016) [16]*	112	97.1	98.7	NA	NA	NA	NA	NA	NA
The present study	102	91.3	100	20	92.9	100	82	88.9	100
Total	4518	77.1	92.0	1115	94.5	64.2	1650	40	95.5

* These 2 studies did not report the acid-fast smear results.

121 respiratory specimens, the sensitivity of Xpert MTB/RIF and Cobas TaqMan was 74.6% and 73.8%, respectively, among culture-positive samples (n=68) [19]. Though our case number was relatively limited, the performance of Xpert MTB/RIF was at least not inferior to that of Cobas TaqMan, and Xpert MTB/RIF offered the advantage of a rapid turn-around time.

The benefit of Xpert MTB/RIF may extend beyond mere diagnosis of TB. Early diagnosis of TB, compared with acid-fast stain and culture, could reduce diagnosis delay, which is crucial in TB control [2]. While assuming that the results of acid-fast stain and Xpert MTB/RIF would be available the same day, the benefit of Xpert MTB/RIF in reducing treatment delay may be most evident among patients with smear-negative TB. The sensitivity of Xpert MTB/RIF, and the proportion of acid-fast smear and culture positivity, will inevitably influence the overall effect and cost-effectiveness of Xpert MTB/RIF in reducing TB diagnosis delay. Our study provided an example of the effectiveness of Xpert MTB/RIF in Taiwan, an intermediate TB burden area. In our patient population, in which only 20% of TB patients had smear-positive pulmonary TB, the application of every Xpert MTB/RIF would likely reduce treatment delay for smear-negative pulmonary TB by 2 days. Our study, therefore, provided useful information regarding the real-world effectiveness of Xpert MTB/RIF in Taiwan.

However, our study has limitations. First, it was not prospective in design. We, therefore, could not ascertain that the quality and quantity of respiratory specimens for Xpert MTB/RIF, Cobas TaqMan, acid-fast smear and culture methods were exactly the same. Second, this was a single center study and the results may need validation before being extrapolated to other hospitals in Taiwan.

In conclusion, our study showed that Xpert MTB/RIF is a useful, rapid point-of-care test for TB diagnosis in Taiwan. Xpert MTB/RIF has high sensitivity and specificity in diagnosing TB. And, Xpert MTB/RIF performance was at least not inferior to that of conventional PCR methods.

References

1. Daley CL. The global fight against tuberculosis. Thorac Surg Clin 2019; 29: 19-25.
2. Lee MR, Lee CH, Wang JY, *et al*. Clinical impact of using fluoroquinolone with low antimycobacterial activity on treatment delay in tuberculosis: hospital-based and population-based cohort study. J Formos Med Assoc 2020; 119: 367-376.
3. Stevens WS, Scott L, Noble L, *et al*. Impact of the GeneXpert MTB/RIF technology on tuberculosis control. Microbiol Spectr 2017; 5.
4. Zhang Q, Sun BQ, Liu C, *et al*. GeneXpert MTB/RIF for rapid diagnosis and rifampin resistance detection of endobronchial tuberculosis. Respirology 2018; 23: 950-955.
5. Bodmer T, Strohle A. Diagnosing pulmonary tuberculosis with the Xpert MTB/RIF test. J Vis Exp 2012: e3547.
6. Horne DJ, Kohli M, Zifodya JS, *et al*. Xpert MTB/RIF and Xpert MTB/RIF Ultra for pulmonary tuberculosis and rifampicin resistance in adults. Cochrane Database Syst Rev 2019; 6: CD009593.
7. Boehme CC, Nabeta P, Hillemann D, *et al*. Rapid molecular detection of tuberculosis and rifampin resistance. N Engl J Med 2010; 363: 1005-15.
8. Steingart KR, Schiller I, Horne DJ, et al. Xpert(r) MTB/RIF assay for pulmonary tuberculosis and rifampicin resistance in adults. Cochrane Database Syst Rev 2014: CD009593.
9. Menzies NA, Cohen T, Lin HH, *et al*. Population health impact and cost-effectiveness of tuberculosis diagnosis with Xpert MTB/RIF: a dynamic simulation and economic evaluation. PLoS Med 2012; 9: e1001347.
10. Lee MR, Huang HL, Chen LC, *et al*. Seroprevalence

of aspergillus igg and disease prevalence of chronic pulmonary aspergillosis in a country with intermediate burden of tuberculosis: a prospective observational study. Clin Microbiol Infect 2020; 26: 1091 e1-1091 e7.

11. Lee MR, Chung KP, Wang HC, *et al*. Evaluation of the Cobas TaqMan MTB real-time PCR assay for direct detection of mycobacterium tuberculosis in respiratory specimens. J Med Microbiol 2013; 62: 1160-1164.
12. Sun HY, Wang JY, Chen YC, *et al*. Impact of introducing fluorescent microscopy on hospital tuberculosis control: a before-after study at a high caseload medical center in Taiwan. PLoS One 2020; 15: e0230067.
13. Yang TL, Lee CM, Lee KL, *et al*. Clinical features of tuberculosis and bacillus Calmette-Guerin (BCG)-associated adverse effects in children: a 12-year study. J Formos Med Assoc 2020.
14. Chiang TY, Fan SY, Jou R. Performance of an Xpert-based diagnostic algorithm for the rapid detection of drug-resistant tuberculosis among high-risk populations in a low-incidence setting. PLoS One 2018; 13: e0200755.
15. Baratloo A, Hosseini M, Negida A, *et al*. Part 1: Simple definition and calculation of accuracy, sensitivity and specificity. Emerg (Tehran) 2015; 3: 48-9.
16. Hsu YM. Evaluation of GeneXpert MTB/RIF assay in a regional teaching hospital, in Taiwan Association of Medical Technologists Conference. 2016.
17. Chou H. An evaluation of rapid molecular tuberculosis identification with the automated GeneXpert MTB/RIF system. Value in Health 2018; 21: S1-S115.
18. Park KS, Kim JY, Lee JW, *et al*. Comparison of the Xpert MTB/RIF and Cobas TaqMan MTB assays for detection of mycobacterium tuberculosis in respiratory specimens. J Clin Microbiol 2013; 51: 3225-7.
19. Antonenka U, Hofmann-Thiel S, Turaev L, *et al*. Comparison of Xpert MTB/RIF with ProbeTec ET DTB and Cobas TaqMan MTB for direct detection of m. Tuberculosis complex in respiratory specimens. BMC Infect Dis 2013; 13: 280.

Squamous Cell Carcinoma Transformation after Acquired Resistance to Osimertinib in a Patient with EGFR-Mutant Lung Adenocarcinoma-Case Report

Zhe-Rong Zheng[1], Gee-Chen Chang[1,2,3*]

Lung adenocarcinoma patients with epidermal growth factor receptor (*EGFR)* mutation usually respond well to EGFR-tyrosine kinase inhibitors (EGFR-TKIs) initially. However, drug resistance will develop eventually. Replacement of threonine by methionine at amino acid position 790 (T790M) at exon 20 of EGFR is the major mechanism of resistance to first- and second-generation EGFR-TKIs, and osimertinib, a third generation EGFR-TKI, can overcome the resistance. Although osimertinib shows an excellent clinical effect in non-small cell lung cancer patients with an EGFR T790M mutation, there are many mechanisms of acquired resistance to it [1]. The point mutation of C797S in exon 20 of EGFR, activating bypass pathways such as MET gene amplification, downstream target activations such as KRAS mutation, PIK3CA mutation, and BRAF mutation, and histologic transformations such as epithelial-to-mesenchymal transition or small cell lung cancer transformation, induce resistance to EGFR inhibitors. We describe a rare occurrence of lung adenocarcinoma with a secondary T790M resistance mutation that transformed into squamous cell carcinoma after acquiring resistance to osimertinib. ***(Thorac Med 2021; 36: 35-40)***

Key words: lung adenocarcinoma, EGFR, squamous cell carcinoma transformation

Introduction

Epidermal growth factor receptor-tyrosine kinase inhibitors (EGFR-TKIs) have a response rate as high as 70~80% and 10~14 months of progression-free survival (PFS) in EGFR-mutant patients [2, 3]. Nevertheless, acquired resistance to EGFR-TKIs will develop eventually. Many mechanisms of acquired resistance to first- and second-generation EGFR-TKIs have been found. The most common is a T790M mutation, which occurs in about 50% of acquired resistance [4]. Osimertinib, a third-generation EGFR-TKI, can overcome T790M resistance. Histological transformation from adenocarcinoma to small cell lung cancer (SCLC) occurs in about 5% of patients receiving EGFR-TKIs [5]. Here, we report a lung adenocarcinoma patient

[1]Division of Chest Medicine, Department of Internal Medicine, Taichung Veterans General Hospital, Taichung, Taiwan
[2]Institute of Biomedical Sciences, National Chung Hsing University, Taichung, Taiwan
[3]Faculty of Medicine, School of Medicine, National Yang-Ming University, Taipei, Taiwan,
Address reprint requests to: Dr. Gee-Chen Chang, Division of Chest Medicine Department of Internal Medicine Taichung Veterans General Hospital 1650 Taiwan Boulevard Sect. 4, Taichung, Taiwan 40705

with transformation to squamous cell carcinoma (SCC) after osimertinib treatment.

Case Report

A 44-year-old male never-smoker suffered from right back pain for 2 months and was referred to our hospital due to a mass lesion at the right upper lung field detected by chest X-ray. Computed tomography (CT) revealed a lobulated mass in the right upper lobe (RUL), 46 x 46 mm in size, and pleural nodules (Figure 1). The whole body bone images obtained using single-photon emission CT/CT (SPECT/CT) with a technetium-99m-diphosphonates (Tc-99m MDP) scanner showed possible bone metastases at the posterolateral aspect of the left-side eighth rib, the spinous process of the L3 spine, and the right iliac bone. The patient underwent sonography-guided core needle biopsy of the lung mass. In the microscopic examination, the cord needle biopsy specimen showed adenocarcinoma, an acinar pattern, and the presence of focal tumor giant cells. Immunohistochemical (IHC) staining revealed the tumor cells were immunoreactive to multi-cytokeratin 1/multi-cytokeratin 3 (AE1/AE3) and thyroid transcription factor-1 (TTF-1), and negative for P40 stains (Figure 2A). There were no keratinizing cells or intracellular bridge, which would indicate the occurrence of squamous differentiation. The EGFR mutation assay showed an exon 19 deletion by MassARRAY genotyping (SEQUENOM). The patient received gefitinib after the EGFR report.

Ten months after gefitinib treatment, the chest CT scan (Figure 1) showed that the primary tumor at the RUL had increased in size,

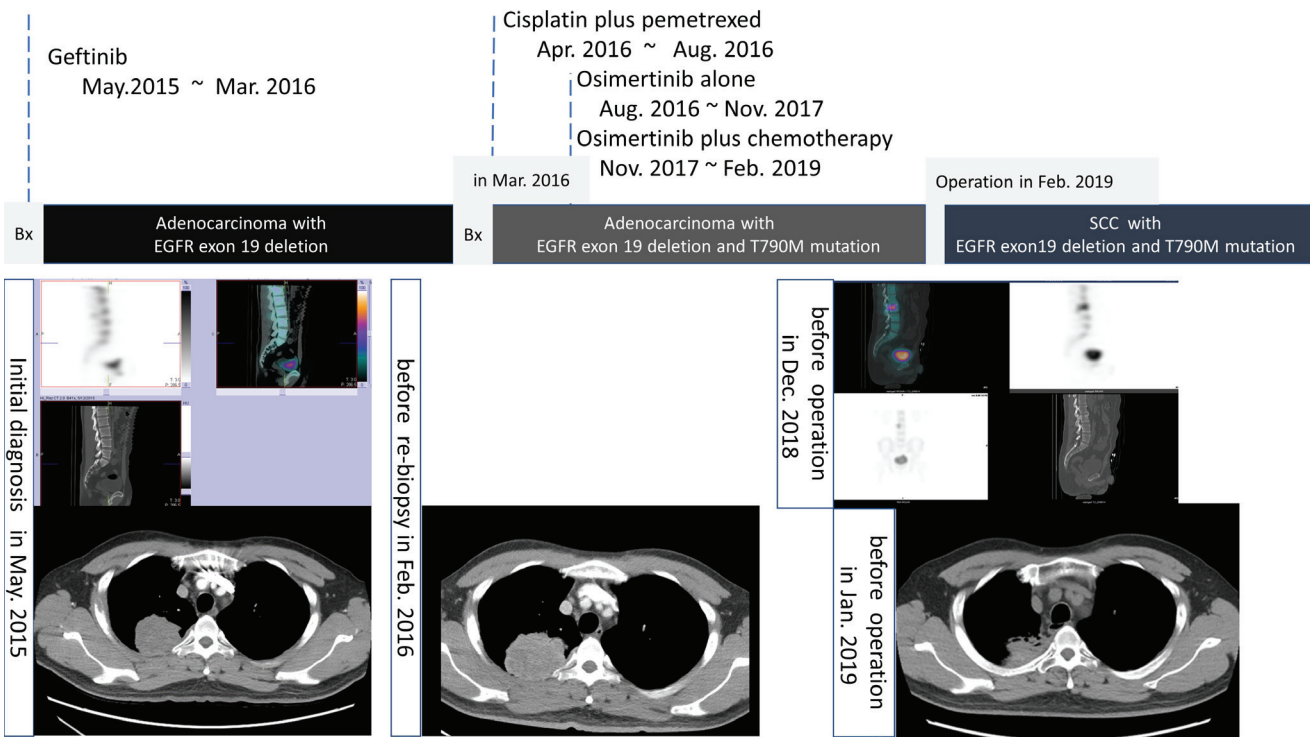

Fig. 1. Timeline of treatment and response evaluation of the chest scan and bone scan. The patient was treated with gefitinib (Iressa™), 6 cycles of cisplatin plus pemetrexed, osimertinib (Tagrisso™), and osimertinib combined with chemotherapy.

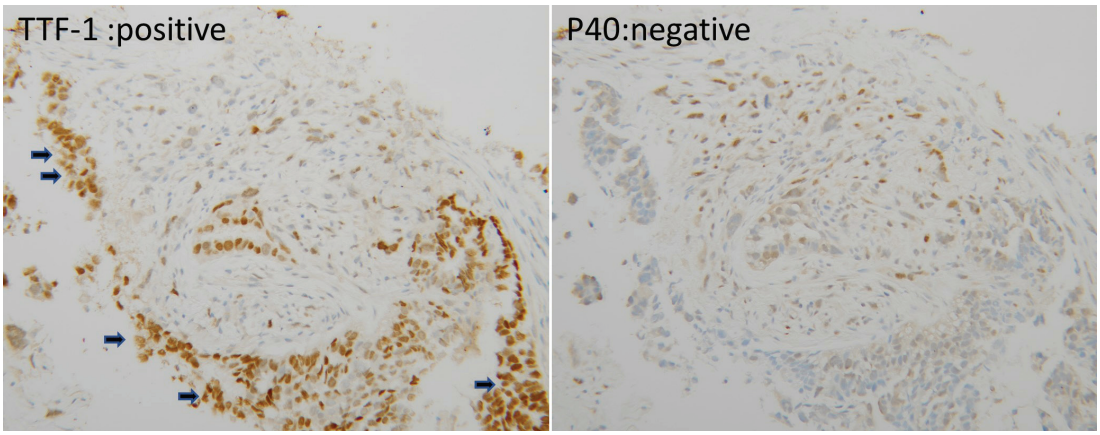

Fig. 2A. Timeline of treatment and response evaluation of the chest scan and bone scan. The patient was treated with gefitinib (Iressa™), 6 cycles of cisplatin plus pemetrexed, osimertinib (Tagrisso™), and osimertinib combined with chemotherapy.

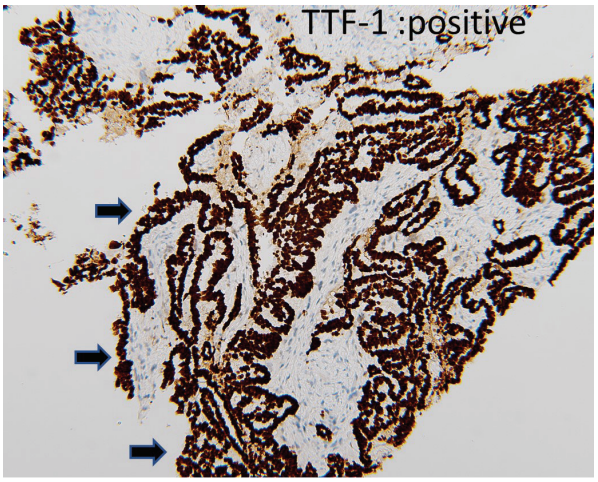

Fig. 2B. After 10 months of gefitinib treatment and with disease progression noted in the chest CT, the pathology report of the core needle biopsy of the lung lesion showed the tumor cells with an acinar pattern were strongly immunoreactive to TTF-1 (arrowhead).

while the whole-body bone scan with Tc-99m MDP showed a stable condition at the bone metastasis sites. We arranged re-biopsy of the primary lung mass, and the IHC stains of the re-biopsied specimen were positive for TTF-1 and p53 overexpression (Figure 2B). The EGFR mutation assay again showed an exon 19 deletion and T790M using MassARRAY genotyping (SEQUENOM). The patient received 6 cycles of chemotherapy with cisplatin plus pemetrexed. Later, the patient was given osimertinib as the next line of treatment with a response duration of 15 months. Imaging study unfortunately revealed mild disease progression and increased carcinoembryonic antigen (CEA) levels were also noted, so we added chemotherapy agents for further treatment. Later, rapid progression of the primary tumor at the RUL was noted on the chest CT scan. Due to progressive lower back pain, a follow-up CT scan was performed which disclosed a new L3 vertebral body metastasis. Posterior total en bloc spondylectomy at L3 with vertebral body replacement was performed for neural decompression and stabilization of spinal instability. The pathological finding of the resected bone and soft tissue specimen revealed metastatic SCC, with keratinization, and the IHC stains were negative for TTF-1 and positive for p40 (Figure 2C). An activating EGFR mutation with an exon 19 deletion and T790M, and without C797S, which was the same as in the recurrent tumor after gefitinib treatment failure, was detected in the SCC tumor. Later, the patient received docetaxel for further treatment. His condition was stable at the time of this writing.

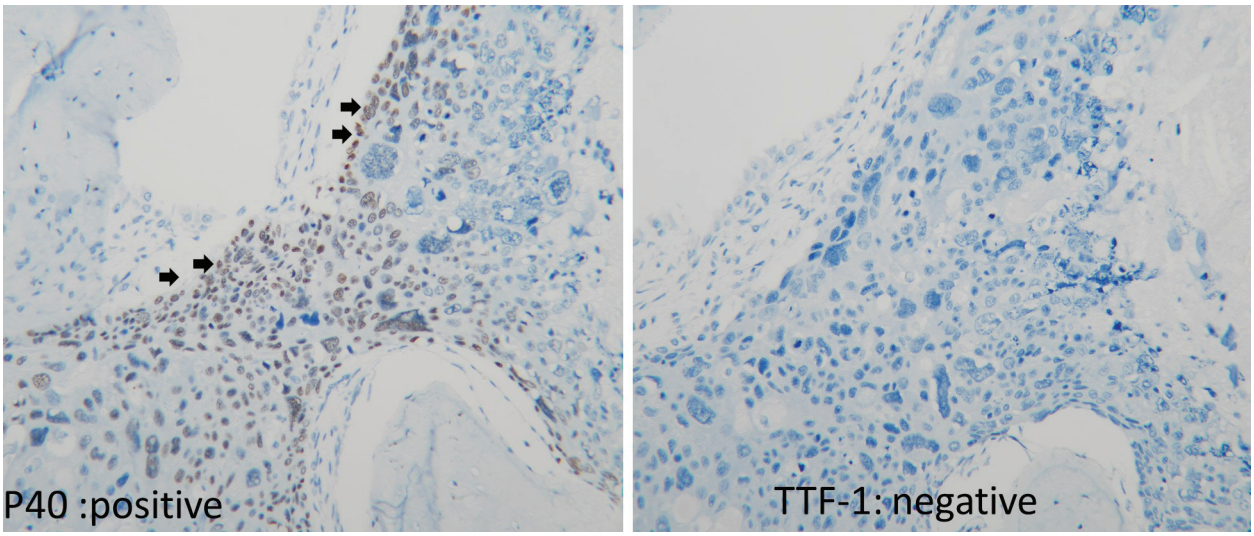

Fig. 2C. After osimertinib treatment and with disease progression noted in the bone scan, the pathology report of the L3 spinal tumor showed the tumor cells with keratinization (arrow) were immunoreactive to P40 (arrowhead) and negative for TTF-1.

Discussion

Numerous mechanisms of drug resistance in patients who take first- and second-generation EGFR-TKIs have been described. Target gene modification, alternative pathways, and histological or phenotypic transformation are 3 of the most common acquired resistance mechanisms [6]. The most common acquired resistance mechanism is T790M. It can alter the binding site of EGFR-TKI, thus reducing the potency of first- and second-generation EGFR-TKIs. Osimertinib, an oral third-generation EGFR-TKI, selectively and irreversibly targets T790M mutations and is the standard treatment for these patients. Although osimertinib has shown excellent clinical effects in NSCLC patients with an EGFR T790M mutation, there are many mechanisms of acquired resistance to it [1]. To start with, the point mutation of C797S in exon 20 of EGFR alters the binding affinity of osimertinib and other mutations such as the L792X mutation, G796S mutation and L718Q mutation, which are novel second-site EGFR mutations leading to drug-resistance. Next, cancer cells can escape the EGFR pathway by activating bypass pathways, such as MET gene amplification, hepatocyte growth factor (HGF) expression and HER2 amplification. In addition, downstream target activations such as the KRAS mutation, PIK3CA mutation, and BRAF mutation continue cell growth and proliferation. Finally, histologic transformation, such as epithelial-to-mesenchymal transition or SCLC transformation, induces resistance to EGFR inhibitors. Lung SCC transformation from EGFR-mutant lung adenocarcinoma is extremely rare.

Our initial tissue was obtained by core needle biopsy, and the possibility of a mixed histology was hard to exclude due to the limited tissue. The patient was treated for EGFR-mutant adenocarcinoma, and spinal metastasis was noted 43 months after treatment. The following surgical pathology showed that the SCC harbored an original exon 19 deletion and T790M, without C797S. This made the possibility of a

second primary tumor unlikely due to the maintenance of the original EGFR mutation after histologic transformation.

To the best of our knowledge, this is the first case report of SCC transformation from adenocarcinoma of the lung after administration of osimertinib in an Asian patient. Seventeen patients with an adenocarcinoma-to-SCC transformation (AST) have been reported, according to a systematic literature review [7]. The median time to AST from TKI start was 11.5 months, and 16 of the 17 patients received first- and second-generation EGFR-TKIs before AST. In our case, we administered gefitinib for the EGFR exon 19 deletion first, and then shifted to chemotherapy after gefitinib failure. Osimertinib was used for the T790M mutation in the re-biopsied tissue. Fifteen months after the initial response, mild progression in the image study and elevation of the tumor marker level were noted. There is no standard therapy after osimertinib failure, and according to standard chemotherapy regimens, combining with osimertinib is tolerable and has a better effect than chemotherapy alone [8], so we subsequently added chemotherapy agents. Furthermore, studies have shown that EGFR-TKI combined with chemotherapy had better PFS and overall survival than EGFR-TKI alone [9-10].

The total duration of osimertinib treatment in our patient prior to AST was 30 months. The existence of the same driver gene mutation in both the original lung cancer and the post-histologic transformation meant that a second primary tumor was unlikely. A previous study showed that AST was mostly found after TKI treatment, and in an animal model, the extracellular matrix remodeling, lysyl oxidase inhibitors, and reactive oxygen species such as phenformin could accelerate the transformation from lung adenocarcinoma to SCC [11]. It appears that an EGFR-TKI-induced change in the tumor microenvironment played a central role in the tumor transformation.

In conclusion, we recommend re-biopsy in cases with tumor recurrence after EGFR-TKI treatment, as transformation into SCLC or SCC with maintenance of the same EGFR mutation that was present in the original adenocarcinoma could occur. The optimal treatment strategy for AST from EGFR-mutant lung cancer has yet to be established, and thus it is essential to accumulate more data with a view to developing an effective treatment.

References

1. Nagano T, Tachihara M, Nishimura Y. Mechanism of resistance to epidermal growth factor receptor-tyrosine kinase inhibitors and a potential treatment strategy. Cells 2018; 7: 212.
2. Tu CY, Chen CM, Liao WC, *et al*. Comparison of the effects of the three major tyrosine kinase inhibitors as first-line therapy for non-small-cell lung cancer harboring epidermal growth factor receptor mutations. Oncotarget 2018; 9: 24237-47.
3. Mok TS, Wu YL, Thongprasert S, *et al*. Gefitinib or carboplatin-paclitaxel in pulmonary adenocarcinoma. N Engl J Med 2009; 361: 947-57.
4. Kobayashi S, Boggon TJ, Dayaram T, *et al*. EGFR mutation and resistance of non-small-cell lung cancer to gefitinib. N Engl J Med 2005; 352:786-92.
5. Sequist LV, Waltman BA, Dias-Santagata D, *et al*. Genotypic and histological evolution of lung cancers acquiring resistance to EGFR inhibitors. Sci Transl Med 2011; 3: 75ra26.
6. Wu SG, Shih JY. Management of acquired resistance to EGFR TKI-targeted therapy in advanced non-small cell lung cancer. Mol Cancer 2018; 17: 38.
7. Roca E, Pozzari M, Vermi W, *et al*. Outcome of EGFR-mutated adenocarcinoma NSCLC patients with changed phenotype to squamous cell carcinoma after tyrosine kinase inhibitors: A pooled analysis with an additional

case. Lung Cancer 2019; 127: 12-18.

8. Neal JW, Hausrath D, Wakelee HA, *et al*. Osimertinib with chemotherapy for EGFR-mutant NSCLC at progression: Safety profile and survival analysis. J Clin Oncol 2019; 37: 9083-9083.
9. Kang J, Li X-M, Cheng J-T, *et al*. The continued osimertinib plus chemotherapy overcoming resistance after histologic transformation in EGFR-mutant lung adenocarcinoma treated with osimertinib. J Clin Oncol 2019; 37: e20615-e20615.
10. Nakamura A, Inoue A, Morita S, *et al*. Phase III study comparing gefitinib monotherapy (G) to combination therapy with gefitinib, carboplatin, and pemetrexed (GCP) for untreated patients (pts) with advanced non-small cell lung cancer (NSCLC) with EGFR mutations (NEJ009). J Clin Oncol 2018; 36: 9005-9005.
11. Hou S, Zhou S, Qin Z, *et al*. Evidence, mechanism, and clinical relevance of the transdifferentiation from lung adenocarcinoma to squamous cell carcinoma. Am J Pathol 2017; 187: 954-62.

Transbronchial Lung Cryobiopsy for Diagnosis of Cytomegalovirus Pneumonia in an Immunocompromised Patient: A Case Report

Shih-Yu Chen[1], Ching-Kai Lin[1], Chao-Chi Ho[1]

Cytomegalovirus (CMV) pneumonia is a common infectious disease in immunocompromised patients. Accurate diagnosis of CMV infection is important to improve the survival rate. We reported a middle-aged man with Henoch-Schonlein purpura under long-term immunosuppressant treatment who had fever and dry cough for 1 week. Chest computed tomography showed multiple peribronchial patches and ground glass opacities in bilateral lungs. Community-acquired pneumonia was considered initially and antibiotics were prescribed, but the chest image and clinical symptoms showed progression. Transbronchial lung cryobiopsy (TBLC) was arranged and CMV pneumonia was confirmed by pathology. There was no adverse event after TBLC and the patient recovered well after anti-viral treatment. To our knowledge, this is the first report on the use of TBLC for diagnosis of CMV pneumonia. ***(Thorac Med 2021; 36: 41-46)***

Key words: cytomegalovirus (CMV) pneumonia, endobronchial ultrasound (EBUS), transbronchial lung cryobiopsy (TBLC), virtual bronchoscopic navigation (VBN)

Introduction

Cytomegalovirus (CMV) infection is common in patients with immunocompromised conditions such as hematologic malignancy, post-hematopoietic stem-cell transplantation, post-solid organ transplantation, human immunodeficiency virus infection, and autoimmune disease, and in those receiving immunomodulating medications [1-3]. Although image pattern, serology study or microbiologic study of a respiratory specimen can be used for diagnosis of CMV pneumonia, surgical lung biopsy remains the gold standard for accurate diagnosis [1, 4-6]. However, surgical lung biopsy cannot be safely performed when patients have respiratory distress and co-morbidities [7, 8]. An alternative diagnostic method with a lower complication rate is needed. Here, we report the first case of a CMV pneumonia patient diagnosed by

[1]Division of Pulmonary Medicine, Department of Internal Medicine, National Taiwan University Hospital, Taipei, Taiwan
Address reprint requests to: Dr. Ching-Kai Lin, Division of Pulmonary Medicine, Department of Internal Medicine National Taiwan University Hospital No. 7, Chung-Shan South Road, Taipei 100, Taiwan

transbronchial lung cryobiopsy (TBLC).

Case Report

A 60-year-old man presented to our hospital with fever for 1 week, accompanied with dry cough and watery diarrhea. There was no associated hemoptysis, chest tightness, abdominal pain, myalgia, arthralgia, or skin eruptions. He had a medical history of Henoch-Schonlein purpura under daily prednisolone 20 mg and mycophenolate mofetil 1000 mg support. On initial physical examination, the patient was ill-looking with a respiratory rate of 20/min, blood pressure of 121/68 mmHg, heart rate of 118/min and body temperature of 36.6 degrees Celsius. Chest auscultation disclosed bilateral coarse breathing sounds. Other examinations, including the cardiovascular, abdominal, central nervous and musculoskeletal system, were unremarkable. Laboratory results showed a normal hemogram, biochemistry, and electrolyte level, except mild anemia with hemoglobin 9.0 g/dL. Initial chest radiograph (CXR) showed ill-defined opacities in bilateral lung fields, especially the upper lung (Figure 1A). Chest computed tomography (CT) disclosed multiple peribronchial patches and ground glass opacities in bilateral lungs. There were also some subpleural opacities and pleural effusion bilaterally (Figure 1B). Bacterial pneumonia or Pneumocystis jiroveci pneumonia was suspected initially; therefore, empiric antibiotics with cefepime and trimethoprim/sulfamethoxazole were administered. However, serial CXR showed progression of the lung parenchymal lesions. Microbiologic studies including bacteria, mycobacteria and fungus yielded negative results and the autoimmune profile revealed no abnormal finding. Histologic proof was suggested as necessary for the final diagnosis and treatment. The patient declined surgical biopsy, and we therefore suggested bronchoscopic biopsy.

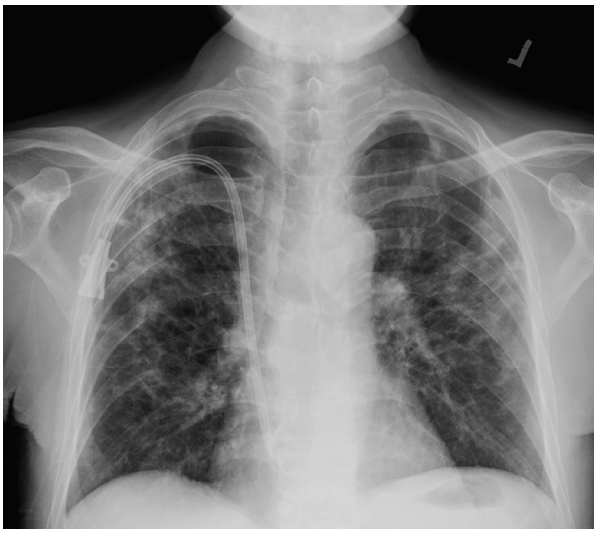

Fig. 1A. Initial chest radiograph revealed bilateral diffuse reticular lesions combined with some consolidations.

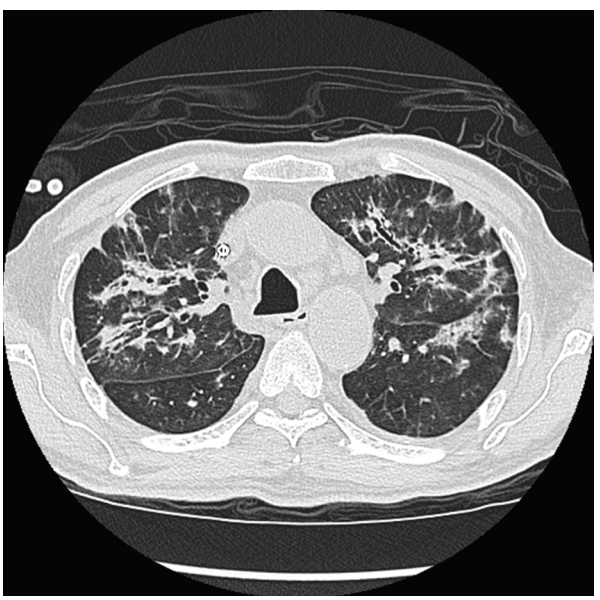

Fig. 1B. Chest computed tomography revealed multiple peribronchial and subpleural patches and peribronchial ground glass opacities in bilateral lungs.

Flexible bronchoscopy (BF-IT260; Olympus Co., Tokyo, Japan) was then performed in a bronchoscopy room setting. After premedication with lidocaine as a local anesthesia, and

with intravenous midazolam and fentanyl for conscious sedation, the scope was inserted through the oral route. We used a commercial navigation planning system (LungPoint® Planner; Broncus Technologies, CA, USA) to select the target lesion and the target bronchus (Figure 2A). The 20 MHz radial endobronchial ultrasound (EBUS) (UM-S20-17S; Olympus Co., Tokyo, Japan) probe was inserted through the working channel of the scope into the target bronchus. A peribronchial lesion with homogenous echogenicity was detected surrounding the right third bronchus under EBUS study (Figure 2B). A 1.9-mm cryoprobe (ERBOKRYO CA, ERBE, Tuebingen, Germany) was then inserted through the working channel of the scope into the target bronchus for TBLC, and carbon dioxide was used as a cooling system. Once brought into position, the probe was cooled for approximately 5–6 seconds, and then was retracted with the frozen lung tissue attached to the probe's tip. The frozen specimen was thawed in saline and then transferred to formalin for fixation. No severe complication was noted after the procedure, except self-limited wound oozing.

The pathologic report revealed scattered cells with large intranuclear inclusion and some intracytoplasmic inclusion in the alveolar lining cells, which were highlighted by CMV immunostaining (Figure 3). The diagnosis of CMV pneumonia was made and the patient was given ganciclovir for 3 weeks without complications. CXR follow-up revealed the bilateral lung opacities were in resolution.

Fig. 2A. The target lesion and target bronchus were localized using a commercialized planning system before the procedure.

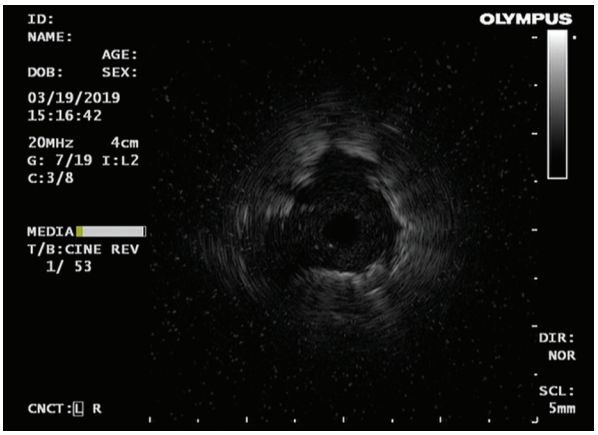

Fig. 2B. Concentric hypoechoic lesions noted under radial EBUS probe at the right 3rd segment.

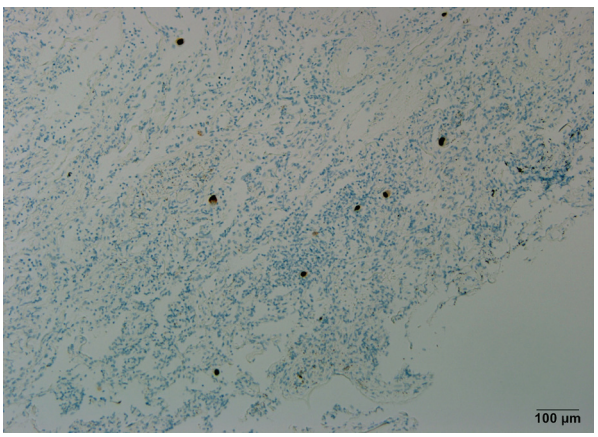

Fig. 3. Inclusion bodies under CMV immunostaining.

Discussion

Accurate diagnosis of CMV pneumonia is important for treatment. The presentation of

clinical symptoms and signs, such as hypoxia, tachypnea, dyspnea or new infiltrates on imaging is generally nonspecific. The CXR or CT imaging pattern is similar to that of connective tissue disease-associated interstitial lung disease or other atypical infections. CMV can be detected from respiratory specimens obtained by expectoration, bronchial washing, or bronchoalveolar lavage (BAL). However, a CMV viral culture is not clinically useful because it takes 2 to 3 weeks to obtain the result [9]. Polymerase chain reaction for CMV (CMV-PCR) is a molecular technique used for identification of the CMV viral load. Some studies reported that CMV-PCR had a sensitivity of more than 90% and specificity of 70~77% in BAL fluid [5, 10-13]. Nevertheless, there is no consensus on the threshold of the CMV DNA (deoxyribonucleic acid) viral load in BAL fluid for use in the diagnosis of CMV pneumonia. There was also a high prevalence of asymptomatic viral shedding [1]. Pathologic diagnosis via lung biopsy is more crucial for this type of patient.

Transbronchial lung biopsy (TBLB) is the conventional method of obtaining a specimen from the lung parenchyma with biopsy forceps. However, the diagnostic accuracy of TBLB was only 29~53% because of the small specimens [7, 14]. In this case, cryobiopsy was used to obtain a better diagnostic yield. Compared to forceps biopsy, cryobiopsy had larger tissue samples (11-15 mm2), less crush artifact and higher diagnostic accuracy (75-80%) for interstitial lung disease [8, 14-16]. The size of the tissue specimen from our patient was 18-21 mm2, and typical histological findings of CMV infection (intranuclear and intracytoplasmic inclusion under CMV immunostaining) were easily obtained. Though there is no report on the use of cryobiopsy for diagnosing CMV pneumonitis, we believe that TBLC could be an alternative choice in this situation.

The most common complications of TBLC are pneumothorax (2-11%) and bleeding (2-25%) [17]. TBLC under fluoroscopy was suggested to avoid pleural injury, and rigid bronchoscopy with an endobronchial blocker has been used to minimize bleeding [14, 18, 19]. However, the tools needed for these 2 procedures are unavailable in most bronchoscopy units in Taiwan. To lower the complication rate in our patient, we incorporated virtual bronchoscopic navigation (VBN) and EBUS for the TBLC procedure. In Ishida`s study, there was high agreement between virtual bronchoscopic images and actual bronchi, enabling the bronchoscope to be inserted more accurately and more peripherally [20]. We used VBN to choose the proper site for biopsy, which was neither too close to the pleura nor accompanied by too many vessels. We also used EBUS for evaluating the detailed information of the target lesion during the procedure. EBUS could also help us avoid the hypervascular area, thereby decreasing the bleeding risk [20-22]. The patient experienced no adverse event (bleeding or pneumothorax) when combining VBN and EBUS during the procedure.

Some experts have advocated surgical lung biopsy for the diagnosis of diffuse lung lesions. The diagnostic yield of TBLC is slightly lower than that of video-assisted thoracoscopic surgery (VATS) lung biopsy (82.8% vs 98.7%) because the median sample size of surgical lung biopsy is larger (46.1±13.8 mm) [17, 23]. Nevertheless, patients that underwent TLBC had a shorter duration of hospitalization (2.6 days vs 6.1 days, $p<0.001$) and lower mortality due to adverse events (2.7% vs 0.3%, $p=0.045$) [17]. TBLC had lower complication and moral-

ity rates, and was also more cost-effective than VATS lung biopsy [8, 15]. VATS lung biopsy could be reserved for patients when a diagnosis is not reached with TBLC.

There is a disadvantage to using TBLC for diagnosis of infectious disease, since frozen samples are not suitable for microbiological studies. The microorganism may not be alive and a frozen section is difficult to culture. In Sanchez-Cabral`s report, more microorganisms could be cultured on BAL samples than on TBLC samples [24]. However, we did not perform BAL for microbiologic culture in this patient. The patient had no fever and no toxic signs at that time, and interstitial lung disease was considered the first priority after multidisciplinary discussion. Without BAL, a misdiagnosis could occur in patients with an infectious disease. The combination of TBLC and BAL might give us more information, helping us to make an accurate diagnosis.

To our knowledge, this is the first case report of CMV pneumonia diagnosed by TBLC. TBLC provides a less invasive, more cost-effective and more definite diagnosis in patients with diffuse lung lesions. It is an alternative choice for patients who decline surgery or who are at high risk with surgical biopsy.

References

1. Dioverti MV, Razonable RR, Cytomegalovirus. Microbiol Spectr 2016; 4. doi:10.1128/microbiolspec. DMIH2-0019-2015.
2. Marchesi F, Pimpinelli F, Ensoli F, *et al*. Cytomegalovirus infection in hematologic malignancy settings other than the allogeneic transplant. Hematol Oncol 2018; 36: 381-91.
3. Siegmund B. Cytomegalovirus infection associated with inflammatory bowel disease. Lancet Gastroenterol Hepatol 2017; 2: 369-76.
4. Uberti-Foppa C, Lillo F, Terreni MR, *et al*. Cytomegalovirus pneumonia in AIDS patients: value of cytomegalovirus culture from BAL fluid and correlation with lung disease. Chest 1998; 113: 919-23.
5. Lodding IP, Schultz HH, Jensen JU, *et al*. Cytomegalovirus viral load in bronchoalveolar lavage to diagnose lung transplant-associated CMV pneumonia. Transplantation 2018; 102: 326-32.
6. Cunha BA. Cytomegalovirus pneumonia: community-acquired pneumonia in immunocompetent hosts. Infect Dis Clin North Am 2010; 24: 147-58.
7. Ramaswamy A, Homer R, Killam J, *et al*. Comparison of transbronchial and cryobiopsies in evaluation of diffuse parenchymal lung disease. J Bronchol Interv Pulmonol 2016; 23: 14-21.
8. Maldonado F, Kropski JA. POINT: Should transbronchial cryobiopsies be considered the initial biopsy of choice in patients with a possible interstitial lung disease? Yes. Chest 2019; 155: 893-5.
9. Wreghitt TG, Teare EL, Sule O, *et al*. Cytomegalovirus infection in immunocompetent patients. Clin Infect Dis 2003; 37: 1603-6.
10. Chemaly RF, Yen-Lieberman B, Castilla EA, *et al*. Correlation between viral loads of cytomegalovirus in blood and bronchoalveolar lavage specimens from lung transplant recipients determined by histology and immunohistochemistry. J Clin Microbiol 2004; 42: 2168-72.
11. Westall GP, Michaelides A, Williams TJ, *et al*. Human cytomegalovirus load in plasma and bronchoalveolar lavage fluid: a longitudinal study of lung transplant recipients. J Infect Dis 2004; 190: 1076-83.
12. Paradis IL, Grgurich WF, Dummer JS, *et al*. Rapid detection of cytomegalovirus pneumonia from lung lavage cells. Am Rev Respir Dis 1988; 138: 697-702.
13. Beam E, Germer JJ, Lahr B, *et al*. Cytomegalovirus (CMV) DNA quantification in bronchoalveolar lavage fluid of immunocompromised patients with CMV pneumonia. Clin Transplant 2018; 32. doi: 10.1111/ctr.13149.
14. Pajares V, Puzo C, Castillo D, *et al*. Diagnostic yield of transbronchial cryobiopsy in interstitial lung disease: a randomized trial. Respirology 2014; 19: 900-6.
15. Hernandez-Gonzalez F, Lucena CM, Ramirez J, *et al*. Cryobiopsy in the diagnosis of diffuse interstitial lung

disease: yield and cost-effectiveness analysis. Arch Bronconeumol 2015; 51: 261-7.
16. Schuhmann M, Bostanci K, Bugalho A, *et al*. Endobronchial ultrasound-guided cryobiopsies in peripheral pulmonary lesions: a feasibility study. Eur Respir J 2014; 43: 233-9.
17. Ravaglia C, Bonifazi M, Wells AU, *et al*. Safety and diagnostic yield of transbronchial lung cryobiopsy in diffuse parenchymal lung diseases: a comparative study versus video-assisted thoracoscopic lung biopsy and a systematic review of the literature. Respiration 2016; 91: 215-27.
18. Babiak A, Hetzel J, Krishna G, *et al*. Transbronchial cryobiopsy: a new tool for lung biopsies. Respiration 2009; 78: 203-8.
19. Pajares V, Torrego A, Puzo C, *et al*. Transbronchial lung biopsy using cryoprobes. Arch Bronconeumol 2010; 46: 111-5.
20. Ishida T, Asano F, Yamazaki K, *et al*. Virtual bronchoscopic navigation combined with endobronchial ultrasound to diagnose small peripheral pulmonary lesions: a randomised trial. Thorax 2011; 66: 1072-7.
21. Asano F, Ishida T, Shinagawa N, *et al*. Virtual bronchoscopic navigation without X-ray fluoroscopy to diagnose peripheral pulmonary lesions: a randomized trial. BMC Pulm Med 2017; 17: 184.
22. Asano F, Shinagawa N, Ishida T, *et al*. Virtual bronchoscopic navigation combined with ultrathin bronchoscopy. A randomized clinical trial. Am J Respir Crit Care Med 2013; 188: 327-33.
23. Romagnoli M, Colby TV, Berthet JP, *et al*. Poor concordance between sequential transbronchial lung cryobiopsy and surgical lung biopsy in the diagnosis of diffuse interstitial lung diseases. Am J Respir Crit Care Med 2019; 199: 1249-56.
24. Sanchez-Cabral O, Martinez-Mendoza D, Fernandez-Bussy S, *et al*. Utility of transbronchial lung cryobiopsy in non-interstitial diseases. Respiration 2017; 94: 285-92.

Pulmonary Lymphomatoid Granulomatosis: A Case Report

Chih-Hung Cheng[1], Yu-Chun Ma[2], Jen-Yu Hung[1,3]

Lymphomatoid granulomatosis (LG), which was first described in the medical literature in 1972, is an uncommon lymphoproliferative disorder that is related to Epstein-Barr virus infection. The lung is the most commonly involved organ, and multiple ill-defined nodules or masses in the middle and lower lobes are its radiologic characteristics. So, pulmonary LG is easily mistaken for lung cancer with bilateral lung metastasis, metastatic tumors, pulmonary tuberculosis, vasculitis, lymphoma, or even sarcoidosis. Here, we reported a case of pulmonary LG. The initial bronchoscopic transbronchial biopsy and transthoracic needle biopsy results could not confirm the diagnosis. Pulmonary LG, grade 3, was finally diagnosed by video-assisted thoracoscopic surgery. After 3 cycles of chemotherapy, the same regimen as for diffuse large B cell lymphoma, improvement in the bilateral multiple pulmonary nodules was remarkable. ***(Thorac Med 2021; 36: 47-51)***

Key words: lymphomatoid granulomatosis, lung lymphoproliferative disorder, Epstein-Barr virus

Introduction

Lymphomatoid granulomatosis (LG) is a rare lymphoproliferative disorder, highly related to Epstein-Barr virus (EBV) infection, and was first described in the medical literature in 1972 [1]. The lung is the most commonly involved organ, and the characteristic radiologic finding of LG is bilateral multiple ill-defined nodules or masses. Thus, pulmonary LG is easily misrecognized as primary lung malignancy, metastatic lung tumor, pulmonary tuberculosis, vasculitis, lymphoma, or even sarcoidosis. It is difficult to confirm the diagnosis using either bronchoscopic transbronchial biopsy or transthoracic needle biopsy. Here, we present the case of a patient with pulmonary LG that was diagnosed by video-assisted thoracoscopic surgery (VATS).

Case Presentation

A 53-year-old male smoker, without chron-

[1]Division of Pulmonary and Critical Care Medicine, Department of Internal Medicine, Kaohsiung Medical University Hospital
[2]Department of Pathology, Kaohsiung Medical University Hospital
[3]College of Medicine, Kaohsiung Medical University, Kaohsiung, Taiwan
Address reprint requests to: Dr. Jen-Yu Hung, Division of Pulmonary Medicine, Department of Internal Medicine National Taiwan University Hospital 16ES, No.100, Tzyou 1st Road, Kaohsiung 807, Taiwan, R.O.C.

Fig. 1. Initial chest X-ray showing bilateral multiple ill-defined pulmonary nodules with middle and lower lobe predominance, and left-side pleural effusion.

ic disease, initially presented with intermittent fever, cough with whitish sputum, hoarseness, and body weight loss. He was transferred to our hospital for bilateral multiple ill-defined lung nodules with left pleural effusion on chest x-ray (Figure 1). Physical examination revealed only decreased breath sounds at the left lower lung field. Mild elevation of C-reactive protein (29 mg/L) was noted; the other laboratory tests were unremarkable. The result of his sputum acid-fast bacillus (AFB) stain was negative. Chest computed tomography (CT) disclosed bilateral multiple ill-defined and variable-sized pulmonary nodules that were lower lobe-predominant and left pleural effusion (Figure 2). Analysis of the left pleural effusion revealed mononuclear cell-predominance (monocyte: 30%; lymphocyte 37%; neutrophil: 32%; mesothelial cell: 1%) and exudative pleural effusion, which indicated a chronic process. Gram's stain and AFB stain of the pleural effusion showed negative results. The cytological study of the pleural effusion was negative for malignant cells.

Initially, bronchoscopic transbronchial tumor biopsy revealed only mild chronic inflammation. Then, CT-guided tumor biopsy revealed only necrotic material. Autoantibody testing for autoimmune disease was weakly positive for anti-Ro antibody (11 EliA U/ml), and the others were all negative. The serum cryptococcal antigen test and galactomannan test were both negative. Finally, to acquire a larger tissue sample for pathology evaluation, left lung wedge resection by video-assisted tho-

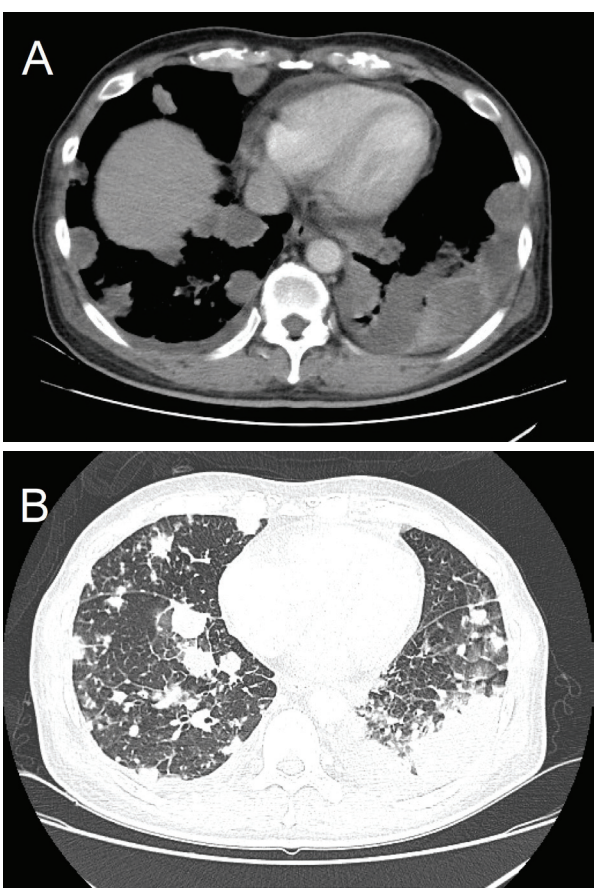

Fig. 2. Chest CT axial view with contrast (A) and high-resolution computed tomography (HRCT) (B) revealing bilateral multiple ill-defined and variable-sized pulmonary nodules with left pleural effusion, without obvious lymphadenopathy.

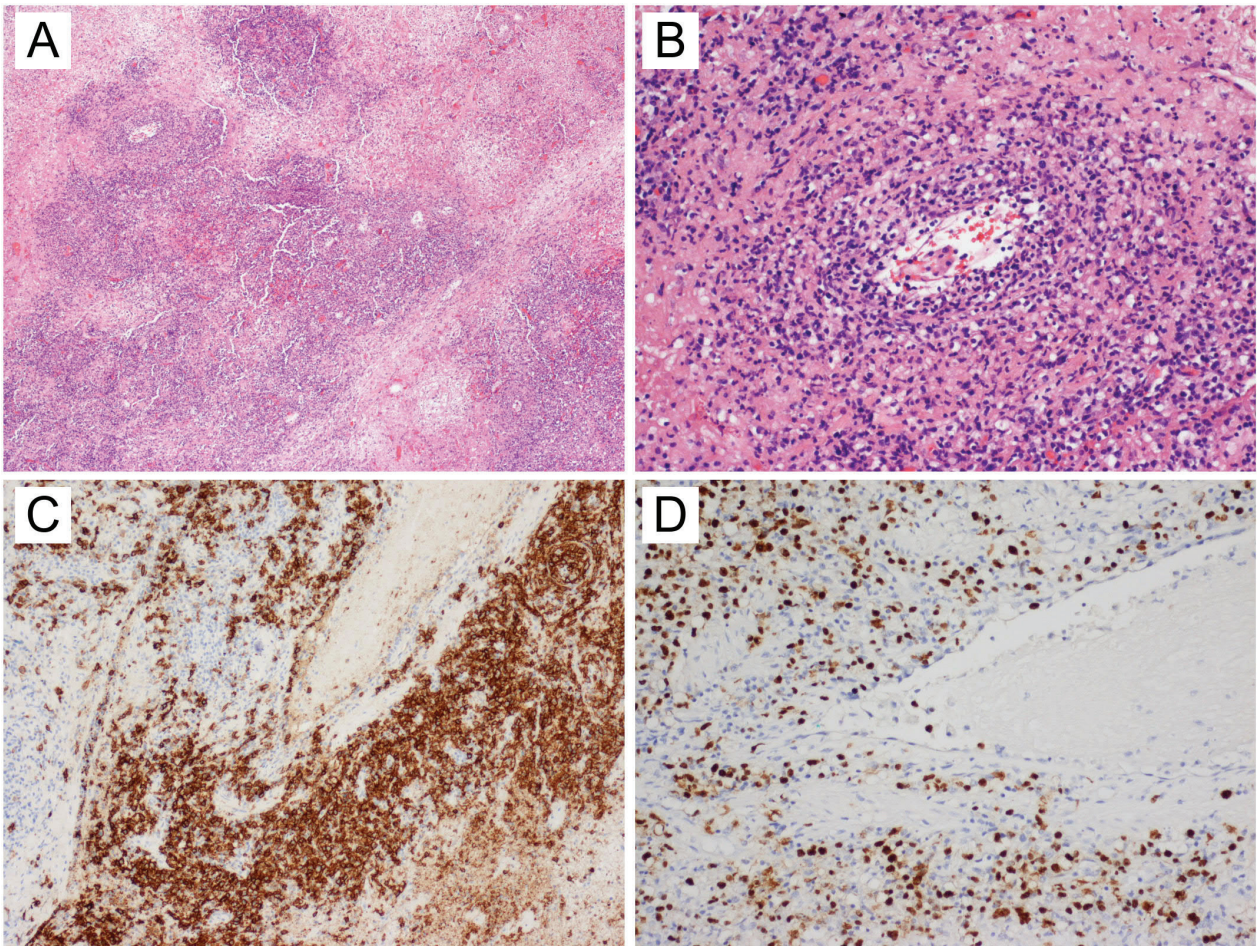

Fig. 1. A Hematoxylin and eosin staining (40X) of the lung resection specimen obtained by VATS shows sheets of mixed, polymorphous atypical lymphoreticular infiltrates with destruction of lung parenchyma and extensive areas of necrosis. B Concentric, transmural infiltration and destruction of the vessel wall is identified (hematoxylin and eosin stain, 200X). C The large atypical cells are positive for CD20 immunohistochemical staining (200X). D Epstein–Barr encoding region (EBER) in situ hybridization (200X) showed more than 50 EBV-positive cells per high-power field.

racoscopic surgery (VATS) was performed. The pathological report (Figure 3) showed polymorphous atypical lymphoid cells infiltration with destruction of lung parenchyma, and transmural concentric infiltration in the media and intima of small- and medium-sized vessels by atypical lymphocytes (EBV-positive cells, > 50 per high-power field), small lymphocytes (CD3 positive T cells), plasma cells, and histiocytes. This pathological finding supported the diagnosis of LG, grade 3. The EBV serological tests, including EBV viral capsid antigen (EB-VCA) and EBV nuclear antigen (EBNA), yielded the following: negative for EB-VCA IgM, positive for EB-VCA IgG, positive for EB-VCA IgA, and positive for EBNA antibody. This finding implied the patient had been infected with EBV in the past, and LG is highly associated with EBV infection. For high-grade (grade 3) and symptomatic disease, chemotherapy with R-CHOP (rituximab, cyclophosphamide, doxorubicin, vincristine, and prednisolone), the same regimen as for diffuse large B cell lymphoma, is suggested. After 3 cycles of chemotherapy

Fig. 4. After 3 cycles of chemotherapy with R-CHOP, the chest x-ray showed remarkable improvement in the bilateral pulmonary nodules.

with R-CHOP, the multiple pulmonary nodules on chest x-ray shrank remarkably (Figure 4).

Discussion

Lymphomatoid granulomatosis (LG) is an uncommon, male-predominant (male-to-female ratio >2:1), lymphoproliferative disorder, which is classified in a family of EBV-associated B cell lymphomas. After LG was first described in 1972 [1], we understood this disease more clearly. Pathologically, LG is characterized as angiocentric polymorphous infiltration by small lymphocytes, plasma cells, and a variable number of large atypical cells. CD3-positive T cells are the majority of the small lymphocytes, and the large atypical cells are usually CD20-positive and EBV-positive B cells [2].

The most commonly involved organ is the lung, followed by the kidney or skin/subcutaneous tissue in different studies [2-4]. Other organs include the central nervous system, peripheral nervous system, liver, spleen, lymph nodes, nasal cavity, gastrointestinal tract, and adrenal gland [2, 3]. The most common symptom of LG is fever, followed by cough, malaise, and body weight loss [5]. Based on the involved organ, neurologic abnormalities or gastrointestinal symptoms may be noted. The characteristic radiological image of pulmonary LG is multiple, poorly-defined pulmonary nodules or masses in the middle and lower lobes, usually bilaterally located. Cavitation may be found by chest CT in a small group of patients [6]. In nonspecific radiological presentations, pulmonary LG can be easily misrecognized as lung cancer with bilateral lung metastasis, metastatic lung tumors, pulmonary tuberculosis, vasculitis (e.g., granulomatosis with polyangiitis, eosinophilic granulomatosis with polyangiitis), lymphoma, or even sarcoidosis [3, 7-9].

With pulmonary LG, VATS or open thoracotomy is usually needed to obtain enough tissue for the diagnosis. The tissue acquired by transbronchial biopsy or transthoracic needle biopsy, like CT-guided biopsy, is usually too small to make an accurate diagnosis. In our case, transbronchial biopsy and transthoracic needle biopsy showed only chronic inflammation or necrosis.

LG is classified into three histological grades, based on the number of EBV-positive atypical B cells. Grade 1 has only scattered EBV-positive atypical B cells (<5 per high-power field), and they might be absent in some cases; 5–20 EBV-positive atypical B cells per high-power field is defined as grade 2; >50 per high-power field is grade 3 [10]. An indolent clinical course is usually noted in grade 1 and grade 2 LG; however, aggressive behavior is

found in grade 3, which is considered to be diffuse large B cell lymphoma [9-10].

The treatment strategy for LG should be based on the use of immunosuppressive agents or not, clinical symptoms severity, and histological grading. Immunosuppressive agents, such as methotrexate or tumor-necrosis factor α inhibitors, should be discontinued as possible. Asymptomatic low-grade (grade 1 and 2) pulmonary LG patients may have only clinical and radiological imaging follow-up without medication. Although interferon-α may be effective in this group, recurrence is frequently noted [3, 10]. Symptomatic high-grade patients should consider chemotherapy using a regimen similar to that for diffuse large B cell lymphoma because of its aggressive behavior, and complete remission may be achieved [10].

Conclusion

Pulmonary LG is an uncommon, male-predominant lymphoproliferative disorder that is highly associated with EBV infection. Its radiological imaging presentation includes multiple ill-defined pulmonary nodules or masses, and pulmonary LG can mimic lung cancer, metastatic tumor, pulmonary tuberculosis, vasculitis, lymphoma, and even sarcoidosis. The lung tissue from transbronchial biopsy or transthoracic needle biopsy is too small for accurate diagnosis of LG. VATS or open thoracotomy is usually needed to obtain enough lung tissue for a definite diagnosis.

References

1. Liebow AA, Carrington CR, Friedman PJ. Lymphomatoid granulomatosis. Hum Pathol 1972; 3: 457-8.
2. Song JY, Pittaluga S, Dunleavy K, *et al*. Lymphomatoid granulomatosis--a single institute experience: pathologic findings and clinical correlations. Am J Surg Pathol 2015; 39: 141-56.
3. Roschewski M, Wilson WH. Lymphomatoid granulomatosis. Cancer J. 2012; 18: 469-74.
4. Sigamani E, Chandramohan J, Nair S, *et al*. Lymphomatoid granulomatosis: A case series from South India. Indian J Pathol Microbiol 2018; 61: 228-32.
5. Katzenstein AL, Carrington CB, Liebow AA. Lymphomatoid granulomatosis: a clinicopathologic study of 152 cases. Cancer 1979; 43: 360-73.
6. Lee JS, Tuder R, Lynch DA. Lymphomatoid granulomatosis: radiologic features and pathologic correlations. AJR Am J Roentgenol 2000; 175: 1335-9.
7. Alexandra G, Claudia G. Lymphomatoid granulomatosis mimicking cancer and sarcoidosis. Ann Hematol 2019; 98: 1309-11.
8. Srivali N, Thongprayoon C, Cheungpasitporn W, *et al*. Lymphomatoid granulomatosis mimicking vasculitis. Ann Hematol 2016; 95: 345-6.
9. Wang R, Lightburn T, Howells J, *et al*. Case-based discussion: a case of misdiagnosis of primary lung malignancy. Thorax 2019.
10. Ok CY, Li L, Young KH. EBV-driven B-cell lymphoproliferative disorders: from biology, classification and differential diagnosis to clinical management. Exp Mol Med 2015; 47: e132.

Primary Pulmonary Epithelioid Hemangioendothelioma Mimicking Lung Metastases: A Clinical Diagnostic Challenge

Chia-Chen Wu[1], Yi-Ming Chang[2], Kai-Hsiung Ko[3]
Hsuan Ying Huang[4], Tsai-Wang Huang[1]

Pulmonary epithelioid hemangioendothelioma is a rare, low-grade malignant tumor of vascular endothelial cell origin. The prevalence of epithelioid hemangioendothelioma is less than 1 in 1 million individuals, and only 12% of cases present as lung disease only. Patients are generally asymptomatic, and the condition occurs more commonly in women. Radiologic images often show multiple, bilateral small lung lesions. However, diagnosis based on clinical and radiological findings is difficult. Histopathological examination is the gold standard. Here, we present a case of primary pulmonary epithelioid hemangioendothelioma that clinically mimicked gallbladder cancer with pulmonary metastases. ***(Thorac Med 2021; 36: 52-59)***

Key words: pulmonary epithelioid hemangioendothelioma, lung metastases, multiple pulmonary nodules

Introduction

Epithelioid hemangioendothelioma (EHE) is a rare vascular, low- to intermediate-grade tumor of endothelial origin [1-4, 10]. Weiss and Enzinger initially applied this term to describe a soft tissue vascular tumor of borderline malignancy [3]. As a low-to-intermediate grade sarcoma, the tumor mostly involves the liver, lungs, soft tissues, and, rarely, the bones; it can be aggressive and multicentric, even resulting in systemic metastasis [5-6]. Pulmonary epithelioid hemangioendothelioma (PEH) was originally described as an intravascular bronchioloalveolar tumor of the lung. It was previously thought to be an aggressive form of bronchoalveolar cell carcinoma [4]. Patients are generally asymptomatic, and the disease occurs more commonly in women and young adults [7-8]. Typical computed tomography (CT) findings include multiple, partially well-circumscribed nodules, multiple pulmonary reticulonodular opacities, and diffuse infiltrative pleural thickening [5]. Diagnosis based on clinical and

[1]Division of Thoracic Surgery, Department of Surgery, Tri-Service General Hospital, National Defense Medical Center, Taipei, Taiwan, R.O.C.
[2]Department of Pathology, Tri-Service General Hospital, National Defense Medical Center, Taipei, Taiwan, R.O.C.
[3]Department of Radiology, Tri-Service General Hospital, National Defense Medical Center, Taipei, Taiwan, R.O.C.
[4]Department of Anatomical Pathology, Kaohsiung Chang Gung Memorial Hospital and Chang Gung University College of Medicine, Kaohsiung, Taiwan, R.O.C.
Address reprint requests to: Dr. Tsai-Wang Huang, Division of Thoracic Surgery, Department of Surgery, Tri-Service General Hospital, National Defense Medical Center, 4F., No. 325, Sec. 2, Chenggong Rd., Neihu Dist., Taipei City 114027, Taiwan (R.O.C.)

radiological findings is difficult. Histopathological examination is the gold standard. Here, we report a patient with primary PEH who was transferred to our department with a diagnosis of gallbladder cancer with multiple pulmonary metastases.

Case report

A 73-year-old previously healthy man and non-smoker visited a local gastroenterology outpatient department with the initial presentation of abdominal fullness lasting 1 year. Enhanced CT of the abdomen (Figure 1) showed asymmetrical wall thickening in the gallbladder body, suggestive of a gallbladder tumor. Multiple bilateral lung nodules, including all lobes, were also noted. He was referred to our general surgery outpatient department where enhanced CT of the chest (Figure 2A, B) revealed multiple circumscribed solid nodules randomly distributed in both lungs, including all pulmonary lobes. These findings were suggestive of secondary pulmonary metastases. There were no enlarged lymph nodes, pleural effusion, or other relevant pulmonary changes. Thus, he was transferred to our thoracic surgery department for lung biopsy under a suspicion of gallbladder cancer with pulmonary metastases.

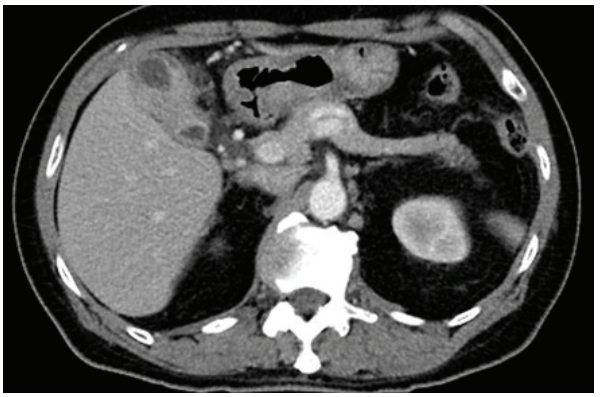

Fig. 1. Abdominal computed tomography revealed asymmetrical wall thickening in the gallbladder body, suggestive of a gallbladder tumor.

Physical examination was unremarkable. Routine laboratory tests were within normal ranges. Serum levels of neoplastic markers revealed elevated carcinoembryonic antigen (CEA) (9.6 ng/mL) and carbohydrate antigen 19-9 (CA 19-9) (70.25 U/mL); squamous cell carcinoma antigen (0.6 U/mL) was within normal range. Preoperative forced vital capacity was 2.81 liters (92.1% of predicted value) and forced expiratory volume in 1 second was 2.5 liters (104.6% of predicted value).

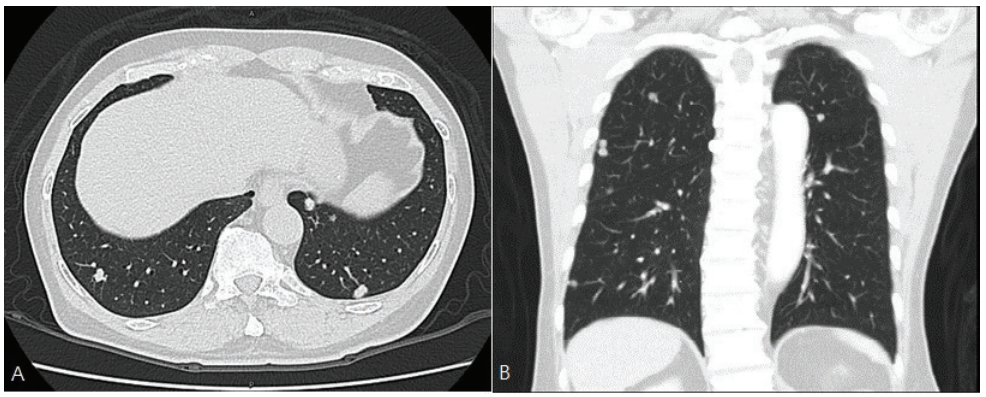

Fig. 2. A. Thoracic computed tomography revealed multiple circumscribed solid nodules randomly distributed in both lungs. **B.** Multiple circumscribed solid nodules randomly distributed in all pulmonary lobes.

Fig. 3. The right lower lobe nodule was palpable, 1 cm in size, hard, and capsulated in nature.

The patient underwent uniportal non-intubated video-assisted thoracic surgery with wedge resection of the right lower lobe of the lung. The right lower lobe nodule was palpable, 1 cm in size, hard, and capsulated in nature (Figure 3). There was no adhesion with the lung parenchyma or pleura. The frozen section showed a grossly mild, firm whitish nodule composed of hypocellular fibrous and chondroid nests, which indicated hamartoma or amyloidosis rather than malignancy. Another wedge resection of the right lower lobe was performed to create a permanent specimen. This examination revealed 3 gray, firm tumor lesions composed of hypocellular epithelioid cells with pale abundant cytoplasm, mild nuclear atypia, and focal vacuolation (Figure 4A). The neoplastic cells were immunoreactive for CD31, CD34, and ERG (Figure 4B, C, D), but negative for cytokeratin, S-100 and SMA. Dual-color break-

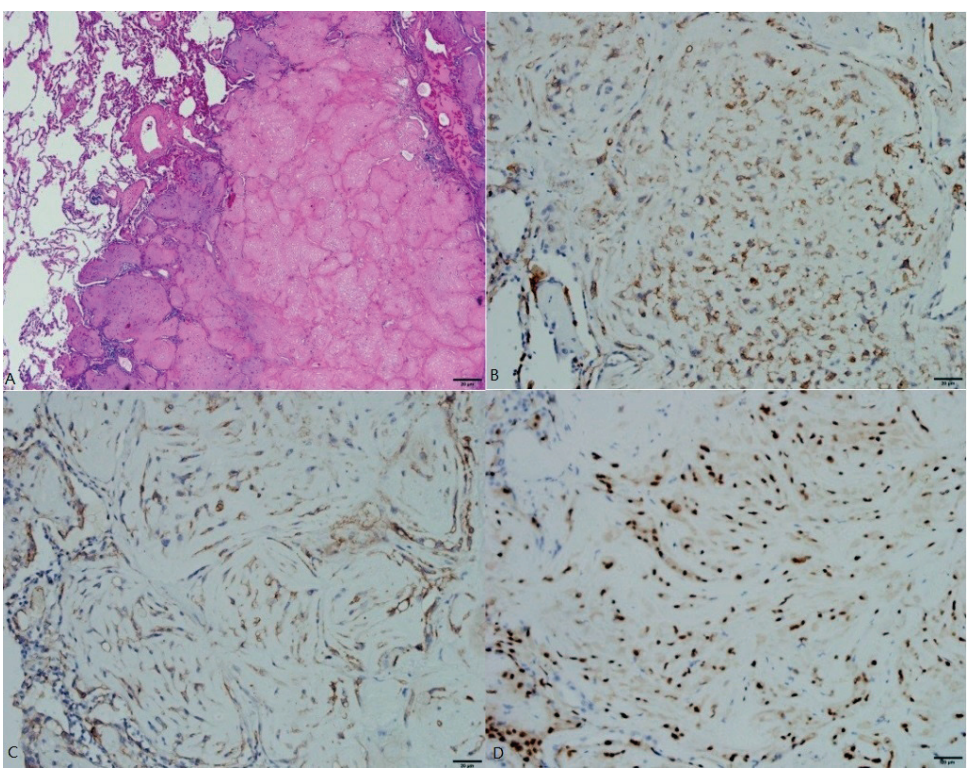

Fig. 4. Pathological findings: (A) The tumor was well demarcated, and the neoplastic cells revealed abundant eosinophilic cytoplasm and bland oval nuclei (hematoxylin and eosin, x 200). These tumor cells were diffusely positive for CD34 (Fig. 4B x 200), CD31 (Fig. 4C x 200) and ERG (Fig. 4D x 200).

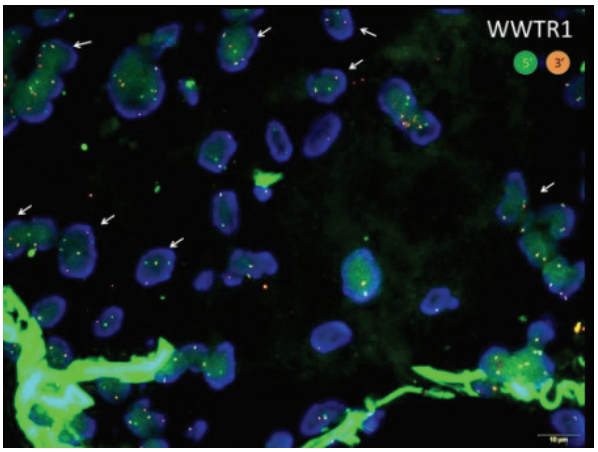

Fig. 5. Dual-color break-apart FISH probes show rearrangements of WWTR1 and CAMTA1. Break-apart signals (split orange and green signals) are present in neoplastic EHE cells, while normal cells contain 2 intact signals (yellow signals).

apart probes of fluorescence in situ hybridization showed rearrangements of WWTR1 and CAMTA1 (Figure 5). The probes are used in pairs. When a chromosome is intact, a yellow signal is observed; when a translocation is present, the 2 probes are split apart, and the individual orange and green fluorescent probes can be visualized. Based on the clinical information, histopathological features, immunoprofiles, and the results of fluorescence in situ hybridization, the patient was diagnosed with EHE.

18F-fluorodeoxyglucose positron emission tomography (FDG-PET) and cholecystectomy of the gallbladder tumor were arranged for proper staging after discussion with a multidisciplinary tumor board. The analysis showed intense FDG-avidity at the gallbladder wall thickening (SUVmax= 11.2, metabolic size > 1.8 cm), suspected of malignancy, and minimal FDG-avidity at multiple nodules in both lungs, suggesting the presence of lung metastases.

Laparoscopic cholecystectomy and wedge resection of the liver revealed chronic cholecystitis with marked congestion without tumor cells. The patient chose regular follow-up rather than chemotherapy because of his age, and the progression of the asymptomatic tumor was slow.

Discussion

PEH was originally described in 1975 as an intravascular bronchioloalveolar tumor of the lung. It was initially thought to be an aggressive form of bronchoalveolar cell carcinoma [4]. The term "epithelioid hemangioendothelioma" was first applied by Weiss and Enzinger to a soft tissue vascular tumor of borderline malignancy in 1982 [3].

EHE is a rare, vascular, low- to intermediate-grade tumor of endothelial origin, according to the 2015 World Health Organization (WHO) classification [1]. The prevalence of EHE is estimated to be less than 1 in 1 million individuals. The most common presentations were liver alone (21%), liver plus lung (18%), bone alone (14%), and lung alone (12%) [2]. Approximately 160 cases of PEH have been reported thus far [9].

Clinical Characteristics of PEH

The incidence of PEH is 2-fold higher in women than in men. It mainly affects young adults, and the median age of onset is 36 years [7-8]. Most patients are asymptomatic. Some patients have minor or nonspecific pulmonary symptoms, such as chest pain, pleuritic pain, cough, sputum, dyspnea, hemoptysis, fever, and weight loss [6-7, 10]. The physical examination is often unremarkable. PEH is often detected in patients without previous symptoms through imaging studies.

The age of our patient was 73 years, which

is much older than the typical age of patients with PEH. In addition, this patient was male, representing the minority of cases. He presented with abdominal fullness in the absence of other pulmonary symptoms. A gallbladder tumor with multiple bilateral lung nodules was incidentally detected, and he was initially diagnosed with gallbladder cancer with pulmonary metastases.

Laboratory Examination Results

Low- to intermediate-grade EHE progresses slowly, so laboratory parameters of most patients show no abnormality. Levels of tumor markers, such as CEA and CA 19-9, were within normal range in previous reports of PEH. Specific markers of EHE in the serum still need to be explored in the future. In this case, elevated levels of CEA (9.6 ng/mL) and CA 19-9 (70.25 U/mL) were found. Malignancy of other origin should also be surveyed. After a series of examinations, including PET and cholecystectomy, other malignancies were excluded.

Radiology Results

The most characteristic feature of CT imaging in patients with PEH is multiple discrete perivascular nodules with well- or ill-defined margins in bilateral lungs. The nodules may range in size up to 3 cm (most are < 1 cm in diameter) [5,11]. This radiological presentation was suggestive of numerous lung diseases including pulmonary metastases, miliary granulomatous infection, sarcoidosis, silicosis, primary lung malignancy, and lymphangitic carcinomatosis; it can be easily misdiagnosed as metastatic carcinoma in an initial interpretation of radiologic findings [15].

Our patient presented with multiple circumscribed solid nodules randomly distributed in both lungs, including all pulmonary lobes, without punctate calcification or pleural indentation. These images resulted in misdiagnosis as metastatic lung cancer.

Differential Diagnosis

EHE can simultaneously or sequentially arise from numerous organs, including the lungs, liver, bone, and soft tissue. Following its occurrence, it may be difficult to determine whether the tumor was multicentric from the beginning or if there was a primary lesion with metastases to other tissues [6]. Disseminated PEH can occur through blood vessels and lymphatics, and within the pleural cavity [16]. When the primary location is the lungs, distant metastases to the liver, skin, kidney, spleen, and retroperitoneum have been reported, although rarely [13, 20].

18F-FDG-PET is an important tool for the diagnosis of PEH [19]. However, a negative PET cannot rule out the presence of PEH [20]. It is important to note that the diagnostic accuracy and reliability of PET-CT decreases when examining multinodular patterns with small lung nodules (diameter: ≤ 20 mm). In our patient, PET showed intense FDG-avidity at the gallbladder wall thickening, suspicious of malignancy, and minimal FDG-avidity at multiple nodules in both lungs, suggesting the presence of lung metastases. The PET analysis also resulted in misdiagnosis as gallbladder cancer with secondary pulmonary metastases.

Pathological Characteristics

The gold standard for diagnosis is histopathological examination and immunohisto-

chemical analysis. Immunohistochemistry staining for vascular-endothelial markers includes CD31, CD34, and factor VIII-related von Willebrand antigen [5]. Other cell markers, such as vimentin, cytokeratin, and EMA are also present in some PEH tumors. [7,21]. Nuclear staining of the ETS family transcription factor ERG is currently among the best available markers of endothelial differentiation, including vascular neoplasms such as hemangioma, hemangioendothelioma, angiosarcoma, Kaposi sarcoma, and EHE [22]. PEH is closely associated with arterioles, venules, and lymphatic vessels, and often displays an intra-alveolar growth pattern [3]. Calcification is commonly observed histologically; typical PEH does not show necrosis, cytological atypia, or a high mitotic index [23]. However, cellular pleomorphism, mitotic activity, necrosis, and extensive cellular spindling are cytologic features that predict aggressive behavior. A recent study recognized the usefulness of WWTR1 and CAMTA1 fusion in the diagnosis of PEH regardless of the clinical profile. EHE is characterized by a t(1;3)(p36;q23-q25) rearrangement, resulting in a WWTR1-CAMTA1 fusion in > 90% of cases [1]. Moreover, Antonescu et al. [24] identified a separate translocation event (YAP1-TFE3) in a subset of EHE with distinct morphological features, which occurred in a specific group of young adults.

In our case, the vascular markers (CD31, CD34, and ERG) and rearrangements of WWTR1 and CAMTA1 undoubtedly indicated PEH.

Prognosis and Treatment

Owing to its low incidence and borderline malignancy features, there is no consensus on therapeutic regimens for the standard treatment of PEH [7]. Surgery should be considered when tumor resection is feasible [25]. Treatment with immunostimulants or chemotherapy with interferon-2α or carboplatin plus etoposide is the preferred therapy for patients with disseminated disease; however, the benefits are unclear [7,17]. Radiotherapy has been proven ineffective because of the radiobiological characteristics of tumors, particularly the slow growth of tumor cells [26]. In asymptomatic patients, spontaneous partial regressions have been reported [13].

The prognosis for patients with this tumor is unpredictable and variable, with survival ranging from < 1 year to 30 years [27]. On the basis of an analysis conducted by Lau et al., the 5-year overall survival is 73% [2]. In a review of 93 patients, it was revealed that male sex, symptomatic disease, pleural effusion, metastases, and lymph node metastases were significant risk factors [12].

Our patient, at 73 years of age, was somewhat older than the typical patient presenting with PEH. Male patients with PEH are also in the minority. Elevated tumor markers such as CEA and CA 19-9, which presented in our case, are rare in patients with PEH. Our patient had asymmetrical wall thickening of the gallbladder and bilateral pulmonary nodules. Given the presence of multiple, small, round pulmonary nodules and elevated tumor markers, we considered the possibility of metastatic nodules. However, the final pathologic finding was indicative of PEH, and the gallbladder tumor was proved to be cholecystitis.

Conclusion

The presence of an unusual primary PEH

in an older male patient, with multiple, bilateral pulmonary solid nodules as CT findings, and elevated tumor markers, which mimicked gallbladder cancer with pulmonary metastasis, indicates the difficulty in diagnosing this rare tumor. Clinicians should consider the possibility of a low-grade malignancy, even if intraoperative frozen analysis reveals benign features. Histopathological analysis is crucial.

References

1. Travis WD, Brambilla E, Nicholson AG, *et al*. The 2015 World Health Organization Classification of Lung Tumors: impact of genetic, clinical and radiologic advances since the 2004 classification. J Thorac Oncol 2015; 10: 1243–60.
2. Lau K, Massad M, Pollak C, *et al*. Clinical patterns and outcome in epithelioid hemangioendothelioma with or without pulmonary involvement: insights from an internet registry in the study of a rare cancer. Chest 2011; 140: 1312–18.
3. Weiss SW, Enzinger FM. Epithelioid hemangioendothelioma: a vascular tumor often mistaken for a carcinoma. Cancer 1982; 50:970–81.
4. Dail DH, Liebow AA. Intravascular bronchioalveolar tumor. Am J Pathol 1975; 78:6–7.
5. Kim EY, Kim TS, Han J, *et al*. Thoracic epithelioid hemangioendothelioma: imaging and pathologic features. Acta Radiol 2011; 52: 161–66.
6. Cronin P, Arenberg D. Pulmonary epithelioid hemangioendothelioma: an unusual case and a review of the literature. Chest 2004; 125: 789–93.
7. Sardaro A, Bardoscia L, Petruzzelli MF, *et al*. Epithelioid hemangioendothelioma: an overview and update on a rare vascular tumor. Oncol Rev 2014; 8(2): 259.
8. Rosenberg A, Agulnik M. Epithelioid hemangioendothelioma: update on diagnosis and treatment. Curr Treat Options Oncol 2018; 19(4): 19.
9. Zheng Z, Wang H, Jiang H, *et al*. Apatinib for the treatment of pulmonary epithelioid hemangioendothelioma: a case report and literature review. Medicine (Baltimore) 2017; 96: e8507.
10. Kitaichi M, Nagai S, Nishimura K, *et al*. Pulmonary epithelioid haemangioendothelioma in 21 patients, including three with partial spontaneous regression. Eur Respir J 1998; 12(1): 89–96.
11. Baba, H., Tomiyasu, M., Makino, H. *et al*. Surgical resection of a primary pulmonary epithelioid hemangioendothelioma in bilateral lungs. Gen Thorac Cardiovasc Surg 2010; 58: 431–33.
12. Amin RM, Hiroshima K, Kokubo T, *et al*. Risk factors and independent predictors of survival in patients with pulmonary epithelioid haemangioendothelioma. Review of the literature and a case report. Respirology 2006 Nov; 11(6): 818-25.
13. Groeschl RT, Miura JT, Oshima K, *et al*. Does histology predict outcome for malignant vascular tumors of the liver? J Surg Oncol. 2014; 109(5): 483–6.
14. Campione S, Cozzolino I, Mainenti P, *et al*. Hepatic epithelioid hemangioendothelioma: pitfalls in the diagnosis on fine needle cytology and "small biopsy" and review of the literature. Pathol Res Pract 2015; 211(9): 702–5.
15. Noh GT, Lee KJ, Sohn HJ, *et al*. Pulmonary epithelioid hemangioendothelioma misconceived as pulmonary metastasis of other malignancies. Yeungnam University J Med 2016; 33(1): 72-5.
16. Weissferdt A, Moran C. Primary vascular tumors of the lungs: a review. Ann Diagn Pathol 2010; 14: 296e308.
17. Bagan P, Hassan M, Le Pimpec Barthes F, *et al*. Prognostic factors and surgical indications of pulmonary epithelioid hemangioendothelioma: a review of the literature. Ann Thorac Surg 2006; 82(6): 2010–2013.
18. Yanagawa H, Hashimoto Y, Bando H, *et al*. Intravascular bronchioloalveolar tumor with skin metastases. Chest 1994; 105(6): 1882–4.
19. Watanabe H, Yano F, Kita T, *et al*. 18F-FDG-PET/CT as an indicator for resection of pulmonary epithelioid hemangioendothelioma. Ann Nuclear Med 2008; 22(6): 521–4.
20. Cazzuffi R, Calia N, Ravenna F, *et al*. Primary pulmonary epithelioid hemangioendothelioma: a rare cause of PET-negative pulmonary nodules. Case Report Med 2011; 2011, Article ID 262674, 6 pages.
21. Shao J, Zhang J. Clinicopathological characteristics of pulmonary hemangioendothelioma: a report of four cases

and review of the literature. Oncol Lett 2014; 8: 2517–22.
22. Miettinen M, Wang ZF, Paetau A, *et al*. ERG transcription factor as an immunohistochemical marker for vascular endothelial tumors and prostatic carcinoma. Am J Surg Pathol 2011; 35(3): 432-41.
23. Mhoyan A, Weidner N, Shabaik A. Epithelioid hemangioendothelioma of the lung diagnosed by transesophageal endoscopic ultrasound-guided fine needle aspiration: a case report. Acta Cytol 2004; 48(4): 555-9.
24. Antonescu CR, Le Loarer F, Mosquera JM, *et al*. Novel YAP1-TFE3 fusion defines a distinct subset of epithelioid hemangioendothelioma. Genes Chromosomes Cancer 2013; 52(8): 775-84.
25. Eguchi K, Sawafuji M. Surgical management of a patient with bilateral multiple pulmonary epithelioid hemangioendothelioma: report of a case. Surg Today 2015; 45(7): 904-6.
26. van Kasteren ME, van der Wurff AA, Palmen FM, *et al*. Epithelioid haemangioendothelioma of the lung: clinical and pathological pitfalls. Eur Respir J 1995; 8(9): 1616-9.
27. Teo SK, Chiang SC, Tan KK. Intravascular bronchioloalveolar tumour. A 20-year survival. Med J Aust 1985; 142(3): 220-2.